Proposal to the Department of Energy,
Office of Basic Energy Sciences,
Division of Engineering

Multiphase Pipelining

Daniel D. Joseph

December 2000

I Research on fundamentals for multiphase pipelining

This proposal focuses on a suite of fundamental problems of multiphase pipelining of liquid-liquid and gas-liquid flows that arise in various branches of the oil industry. We have defined and developed methods of solution to the problems being proposed here. All these problems are academically viable and all are relevant to improvements in the production and transport of oil and gas.

Three broad categories of study will be undertaken.

(1) Analysis of the lubrication efficiency of core-annular flow of heavy oil in turbulent water. The organizing concept introduced here is the friction factor efficiency ratio, which is the ratio of the friction factor for core-annular flow to the friction factor of turbulent flow of water alone at the same superficial velocity. This ratio is greater than one due to extra dissipation that we believe is due to wave propagation on the oil core and fouling. The problem of increased dissipation can be studied theoretically using a turbulence model we have adapted for this application. Using this model, various causes for increased dissipation can be examined one at a time and compared with observed increases of dissipation in laboratory experiments and Syncrude's commercial line. A very large increase in temperature (over 50°C) due to frictional heating in pipelining of bitumen froth was observed in 1" pipes, but not in the 36" commercial pipeline. The problem of frictional heating in turbulent core annular flow has not been studied; there does not seem to be a literature on frictional heating in turbulent pipelines even when only one phase is present; we intend to create such a literature.

(2) Studies of pipelining of gas-liquid flows. We will study stability and bifurcation of stratified flow using a new approach based on viscous potential flow. This transition and pressure drop in annular gas-liquid flow will be studied using our turbulence model looking again at the friction factor efficiency ratio, which here is the ratio of the friction factor of turbulent annular gas-liquid flow to turbulent gas flow when no liquid is on the wall. The huge experimental literature on annular flows can also be processed for understanding the sources of increased dissipation. Preliminary studies suggest that the dissipation increases sharply with the volume fraction of liquid on the wall.

(3) Experimental and numerical studies will be undertaken to explain anomalous properties of Taylor bubbles of gas in water and heavy oils in vertical pipes and in the annulus between concentric vertical cylinders. The numerical studies will be carried out with a fully 3D code based on level set methods that can be applied even to nonaxisymmetric bubbles, which are always observed in annular pipes.

II Accomplishments of our previous DOE/DE-FG02-87ER 13798, 9/1/98--8/31/01

The projects proposed were focused on self-lubricated transport of bitumen froth. This project was brought to us by Syncrude Canada at a time when they were evaluating options for transporting bitumen froth from a newly opened Aurora mine 35 kilometers to the upgrading facility at Lake Mildred. Bitumen froth is a stable water in oil emulsion which is created from the oil sands by a steam process in which most of the dirt and stones are removed. It is extremely important that the natural water left in this emulsion is a colloidal dispersion of clay particles that can be seen as the milk colored white fluid in figure 8. We found that the clay particles are crucial to the success of the technology since they stick to the bitumen yet are hydrophilic, thus giving rise to a surfactant action that acts to keep the clay-covered bitumen from sticking to itself. After the water

coalesces into a lubricating film under shear, the oil on the wall is protected from the buildup of fouling by the clay covering.

Very interesting fundamental problems came out of our DOE/Syncrude studies. We discovered a scale up law in which the friction factor vs. Reynolds number follows the Blasius turbulence relation in which the pressure gradient is proportional to the ratio of the $7/4^{th}$ power of the velocity to the $5/4^{th}$ power of the pipe radius at a cost of ten to 20 times greater than water alone. These results were shown to hold 1", 2" and 24" pipes in the paper by Joseph, Bai, Mata, Grant and Sury, "Self-lubricated transport of bitumen froth", *J. Fluid Mech*. **386**, pp 127-149 1999. Grant and Sury are from Syncrude. Sanders at Syncrude research in Edmonton confirmed the scale up law; together we developed a froth rheometer to determine critical stress for self-lubrication and we found that cement lined pipes promote self-lubrication of bitumen froth because the clay in the natural water promotes a strong wetting of cement by colloidal clay.

The Blasius scale up seems to be universal for lubricated flows in which the lubricating water layer is turbulent. The increased friction is apparently due to waves. The source of the increased friction is a topic of research because unlike roughness, which increases the exponent from 7/4 toward 2, the increase of friction in lubricated flows does not change the exponent.

Based on our joint works with Syncrude people, Syncrude's management authorized a 76 million dollar investment for the construction of a 36" pipeline to run 35 kilometers from the Aurora mine to the upgrading facility at Lake Mildred. The engineering of this pipeline follows our scale up, since no tests were done in such a large pipeline. This line was put into operation in August of 2000; it is a total success and transports froth at a cost 6 times more than water alone, better than expected.

In their press release of August 17, 2000 titled, "**Syncrude's Aurora Mine Heralds New Era of Energy Production for Canada**, *New technology lowers cost and improves environmental performance*," they coin the words "natural froth lubricity":

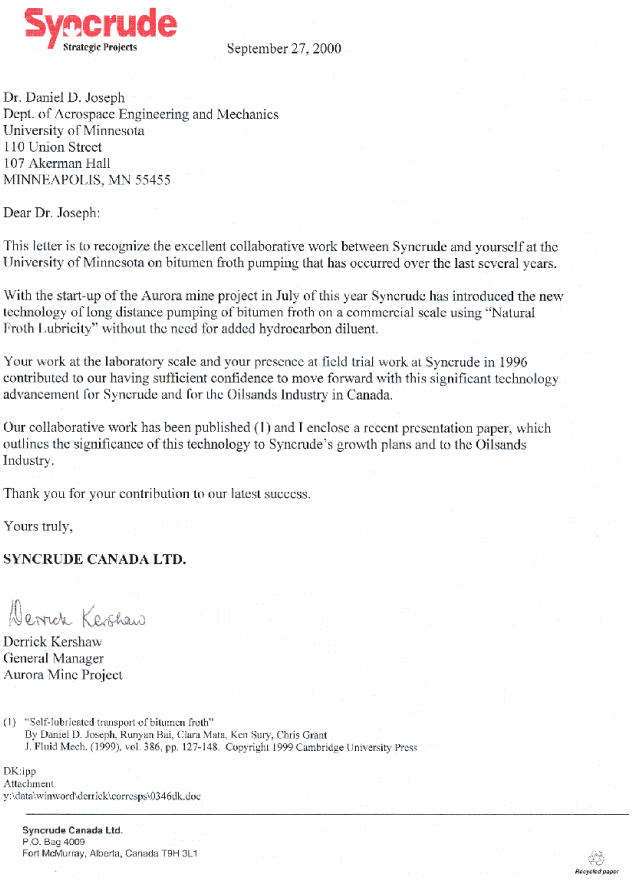

Syncrude
Strategic Projects

September 27, 2000

Dr. Daniel D. Joseph
Dept. of Acrospace Engineering and Mechanics
University of Minnesota
110 Union Street
107 Akerman Hall
MINNEAPOLIS, MN 55455

Dear Dr. Joseph:

This letter is to recognize the excellent collaborative work between Syncrude and yourself at the University of Minnesota on bitumen froth pumping that has occurred over the last several years.

With the start-up of the Aurora mine project in July of this year Syncrude has introduced the new technology of long distance pumping of bitumen froth on a commercial scale using "Natural Froth Lubricity" without the need for added hydrocarbon diluent.

Your work at the laboratory scale and your presence at field trial work at Syncrude in 1996 contributed to our having sufficient confidence to move forward with this significant technology advancement for Syncrude and for the Oilsands Industry in Canada.

Our collaborative work has been published (1) and I enclose a recent presentation paper, which outlines the significance of this technology to Syncrude's growth plans and to the Oilsands Industry.

Thank you for your contribution to our latest success.

Yours truly,

SYNCRUDE CANADA LTD.

Derrick Kershaw

Derrick Kershaw
General Manager
Aurora Mine Project

(1) "Self-lubricated transport of bitumen froth"
By Daniel D. Joseph, Runyan Bai, Clara Mata, Ken Sury, Chris Grant
J. Fluid Mech. (1999), vol. 386, pp. 127-148. Copyright 1999 Cambridge University Press

DK:jpp
Attachment
y:\data\winword\derrick\corresps\0346dk.doc

Syncrude Canada Ltd.
P.O. Bag 4009
Fort McMurray, Alberta, Canada T9H 3L1

Recycled paper

> Long distance pipelining of bitumen froth is enabled by Natural Froth Lubricity. This technology uses the water that is naturally evident in the froth to form a lubricating 'sleeve,' thus allowing the froth to travel via pipeline without adding a diluent such as naphtha.

A letter of recognition of the importance of our contribution to the Aurora project appears above.

The idea of a lubricated gas-liquid flow was proposed by Bannwart and Joseph 1996. We are speaking of annular gas-liquid flow in which the liquid covers the pipe wall. We proposed to think of this flow as lubricated; though the molecular viscosity of the gas is much lower than the eddy viscosity of the turbulent gas is larger. This theory works extremely well for water, both in horizontal and vertical pipes but it is not in such good agreement with data from other liquids. We believe that the basic and new idea that the stabilization of annular flow is due to the increased flow resistance of the turbulent gas is sound and we are going to see if we can come up with an acceptable modification of our theory which is compatible with all the data.

Our studies of the lubricated transport of slurries have been carried out using direct numerical simulation. We have become world leaders in this kind of work and will be able to exploit these new opportunities in the next years. Our main work in this arena during the last year focused on surgical analysis of the inertial, normal stress, shear thinnings and combined effects on the migration of neutrally buoyant particles in Poiseuille flow.

We were recently funded by Exxon-Mobil to do small studies of the lubrication options for a new pipeline they are going to build in Africa.

I have listed the papers that are most relevant to our ongoing work as described here below:

Lubricated Transport

1. A. Bannwart and D.D. Joseph, 1996. “Stability of annular flow and slugging” *Int. J. of Multiphase Flow* **22** (6), 1247-1254.

2. D.D. Joseph, 1997. “Steep wave fronts on extrudates of polymer melts and solutions: Lubrication layers and boundary lubrication”, *J. Non-Newtonian Fluid Mech*., **70**, 187-203.

3. G. Nunez, H. Rivas, D.D. Joseph, Oct. 26, 1998. Drive to produce heavy crude prompts a variety of transportation methods. *Oil and Gas Journal*, 59-68

4. D.D. Joseph and R. Bai, 1999. Interfacial Shapes in the Steady Flow of a Highly Viscous Dispersed Phase. *Fluid Dynamics at Interfaces Ed. Wei Shyy, Cambridge University Press.*

5. D.D. Joseph, R. Bai, C. Mata, K. Surry and C. Grant, 1999. Self Lubricated Transport of Bitumen Froth. *J. of Fluid Mech*., **381**, 127-149

6. R. Bai and D.D. Joseph, 1999. Steady flow and interfacial shapes of a highly viscous dispersed phase. *Int. J. Multiphase Flow*, **26** (8)

7. P. Huang and D.D. Joseph, 2000. "Effects of shear thinning on migration of neutrally buoyant particles in pressure driven flow of Newtonian and Viscoelastic fluids", *J. Non-Newtonian Fluid Mech*., **90**, 159-185.

8. C. Mata, M.S. Chirinos, M.E. Gurfinkel, G.A. Núñez and D.D. Joseph, 2001. "Pipeline transport of highly concentrated oil in water emulsions." SPE paper, to appear.

9. S. Sanders, R. Bai and D.D. Joseph. "Self lubricated transport of bitumen froth; effect of bulk property change and internal pipe coatings." Under preparation.

10. T.A. Smieja, D.D. Joseph, G. Beavers, 2000. "Flow charts and lubricated transport of foams," *Int. J. Multiphase Flow*, submitted.

Honors and awards since 1997 (grant start year):

- Illinois Institute of Technology Professional Achievement Award, 1998
- Kovasznay Lecturer, University of Houston, Mechanical Engineering, April 1999
- University of Chicago, Professional Achievement Award, May 1999
- Fluid Dynamics Prize of the American Physical Society, November, 1999

Patents obtained:

- US Patent 5,988,198. Process for pumping bitumen froth through a pipeline. O. Nieman, K. Sury, D.D. Joseph, R. Bai and C. Grant.

III Lubricated transport of viscous oils. Friction factor efficiency ratio.

The usual notion of lubrication of a solid carries over to the lubrication of a very viscous liquid by a less viscous one. Nature's gift is that the less viscous liquid migrates into regions where the shear is greatest, minimizing dissipation, lubricating the flow. In many of the practical cases, and all those considered here, water lubricates oil. In pipe flows the region of high shear is at the pipe wall, which is where the water migrates. Lubricated flow is hydrodynamically stable, if the oil doesn't stick to the wall and then stick to itself building up fouling, water will go to the wall stably. In the best cases the pressure gradients used to drive water-lubricated flows can be even less than those needed to transport water alone. This can lead to pressure gradient reductions of the order of the viscosity ratio, which can be factors of the order 10^5.

There are three ways to create a water lubrication of oils: (1) core annular flows, in which oil and water are pumped simultaneously, (2) self-lubricated flow of water in oil emulsions, in which the droplets of water are in a thermodynamically stable range, say 30%-40% and form a lubricating layer suddenly, at a critical rate of shear, (3) lubricated flow of concentrated oil in water emulsions, in which lubrication is achieved by

migration of oil droplets away from the wall wringing water out of the core of the emulsion.

All three modes of lubrication have been used in pipelining, depending on local conditions.

The science and technology of core-annular flows, in which oil and water are pumped simultaneously, has a long history since the early 1900's, which is reviewed by Joseph & Renardy 1992[11] and Joseph, Bai, Chen and Renardy 1997[12].

Core-annular flows can be established only in oils of viscosity greater than 500 cp (rule of thumb with some theoretical backup.)

The main threats to core annular flow are

(i) **Stratification.** When the density difference of oil-and water is large, or when the flow is very slow. It takes inertia associated with waves to levitate the core away from the wall.

(ii) **Fouling.** There are *two parts* to fouling. The oil may stick to the wall; this is an energy effect and it depends on the oil and pipe wall interaction measured by contact angles. If the wall is oleophobic, it won't foul and the hydrodynamics will put the water on the wall.

More important than fouling is *buildup of fouling*. Here we know that the wall fouls and we ask if the oil wants to stick to itself; if it does, we will get a buildup of fouling and failure. This depends on the oil and what's in the water. With the right choice of surfactants we might prevent an oil from sticking to itself.

Self-lubricated flow of water in oil emulsions does not require separate pumping of oil and water. Little water droplets of modest volume fraction, say 20% or 30%, are dispersed throughout the oil. The viscosity of this dispersion is even larger than the oil alone. To get lubrication you need to break the emulsion by shearing at the wall (see Kruka 1977)[13]. This implies that there is a critical speed at which the shear becomes large enough to break the emulsion.

We plotted up the data in Kruka's patent; it is displayed as figure 1.

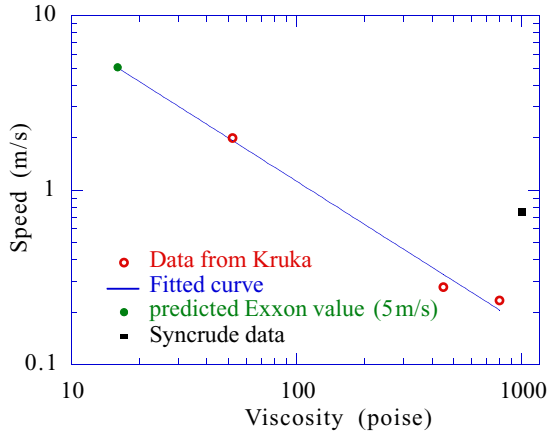

Figure 1. Kruka's data is for 90/10 o/w emulsion using Midway Sunset crude in a 1/2" pipeline. We predict 5 m/sec are required to break 70/30 o/w emulsion.

There is almost no literature on self-lubrication of water in oil emulsions. Besides Kruka's patent, there are reports of self-lubrication of Syncrude's bitumen froth, which is an emerging technology. Syncrude's case is special because the clay in the natural water keeps the oil from sticking to itself; we call this powdering the dough. The patent for this pumping process is described by Neiman *et al* 1999[14].

Syncrude Canada Ltd. contacted us in 1994 to study self-lubrication of bitumen froth. They were particularly interested in fouling as a possible show stopper for self-lubricated pipelining which in-house 1985 studies of O. Nieman[15] suggested might be a viable option for pipelining froth from the mine. Our studies showed that though the pipelines fouled initially, no buildup of fouling would occur. Results of our studies of start and restart of a stopped line were similarly successful. Motivated by the success of the Minnesota studies, Syncrude built a 24"× 1km pilot loop in Fort McMurray. The results of these tests confirmed the Minnesota studies and they provided a database from which we determined a powerful scale-up result described in the abstract[16] partly reproduced here:

> "Bitumen froth is produced from the oil sands of Athabasca using the Clark's Hot Water Extraction process. When transported in a pipeline, water present in the froth is released in regions of high shear; namely, at the pipe wall. This results in a lubricating layer of water that allows bitumen froth pumping at greatly reduced pressures and hence the potential for savings in pumping energy consumption. Experiments establishing the features of this self-lubrication phenomenon were carried out in a 1" diameter pipeloop at the University of Minnesota, and in a 24" (0.6m) diameter pilot pipeline at Syncrude, Canada. The pressure gradient of lubricated flows in 1"(25mm), 2"(50mm) and 24"(0.6m) pipes diameters closely follow the empirical law of Blasius for turbulent pipe flow; the pressure gradient is proportional to the ratio of the 7/4th power of the velocity to the 4/5th power of the pipe diameter, but the constant of proportionality is about 10 to 20 times larger than that for water alone… "

The Blasius expression for a single fluid with viscosity μ, density ρ, velocity U, pressure gradient $\beta = \Delta P/L$ in a pipe of radius R can be written as

$$\beta = 0.316\psi\left\{\frac{\rho^3\mu}{2^9}\right\}^{1/4}\frac{U^{7/4}}{R^{5/4}} \qquad (1)$$

where ψ is the friction factor efficiency ratio, the ratio of the friction factor in two-phase flow to the friction factor for water and gas alone; $\psi = 1$ is for the flow of a single fluid. It is well known and at first surprising that in ideal lubrication in which the core is very viscous, without waves, and the flow of water is laminar, then for a given volume flux the pressure gradient can be smaller than for water. Equation (1) does not apply to laminar flow but an equivalent formula, linear in the mean velocity, would yield a high efficiency with $\psi < 1$. The presence of waves and fouling increase ψ. When dealing with turbulent annular flow, even with turbulent gas-liquid annular flow, it is important to know the value of ψ and how ψ depends on parameters.

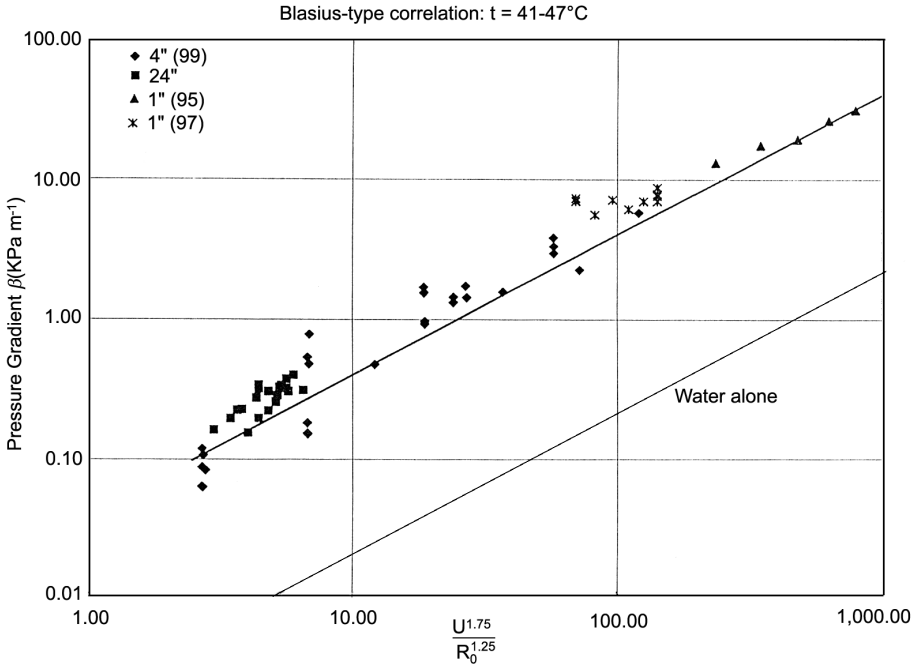

Figure 2. Curve fits parallel to the Blasius correlation for turbulent pipe flow (water alone), for temperature range 41-47°C. [14]

For Syncrude froth in the pilot pipelines mentioned in the abstract ψ is between 10 and 20, and depends strongly on temperature (figure 2). In the 36" commercial line that was designed using the relation (1), the value of ψ is about 6, indicating more efficient lubrication.

The various components of our study of turbulent annular flow can ultimately be expressed in terms of factors that determine the two-phase flow function ψ. This function takes values rather larger than 1 due to fouling of the walls. When the oil on the wall is protected from the buildup of fouling, as in the case of froth covered by clay, waves on the pipe are also driven by turbulent water at a cost in the pressure gradient reflected in the multiplicative factor $\psi > 1$. This increased friction is not like a rough pipe in which the

exponent n ($7/4 \le n \le 2$) of U^n is increased over 7/4 rather than in a multiplicative factor like ψ.

IV Numerical simulation of laminar wavy core flow

Analysis of problems of levitation, transitions between flow types, pressure gradients and hold-up ratios have been carried out by direct numerical simulation. Bai, Kelkar and Joseph[17] 1996 did a direct simulation of steady axisymmetric, axially periodic CAF, assuming that the core viscosity was so large that secondary motions could be neglected in the core. They found that wave shapes with steep fronts like those shown in Figure 3 always arise from the simulation, see figure 4. The wave front steepens as the speed increases. The wave shapes are in agreement with the shapes of bamboo waves in up-flows studied by Bai, Chen and Joseph[18] 1992. Better agreements were obtained by the perturbation analysis for steady flow of a highly but not infinitely viscous core of Bai and Joseph[6] 1999 in which account is taken of flow motions in the core. Li and Renardy[19] 1999 were the first to solve the initial value problem for computed bamboo waves in vertical core annular laminar flow using a volume of fluid method. Their results are in excellent agreement with experiments of Bai *et al* 1992. They found an unsteady solution in which the velocity and pressure in the water change with time but the interfacial shapes are steady.

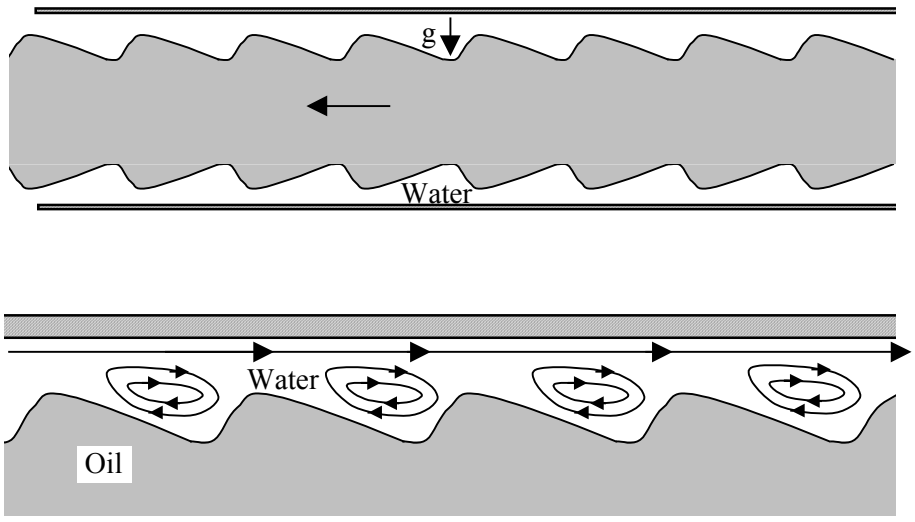

Figure 3. The high pressure at the front of the wave crest steepens the interface and the low pressure at the back makes the interface less steep. The pressure distribution in the trough drives an eddy in each trough.

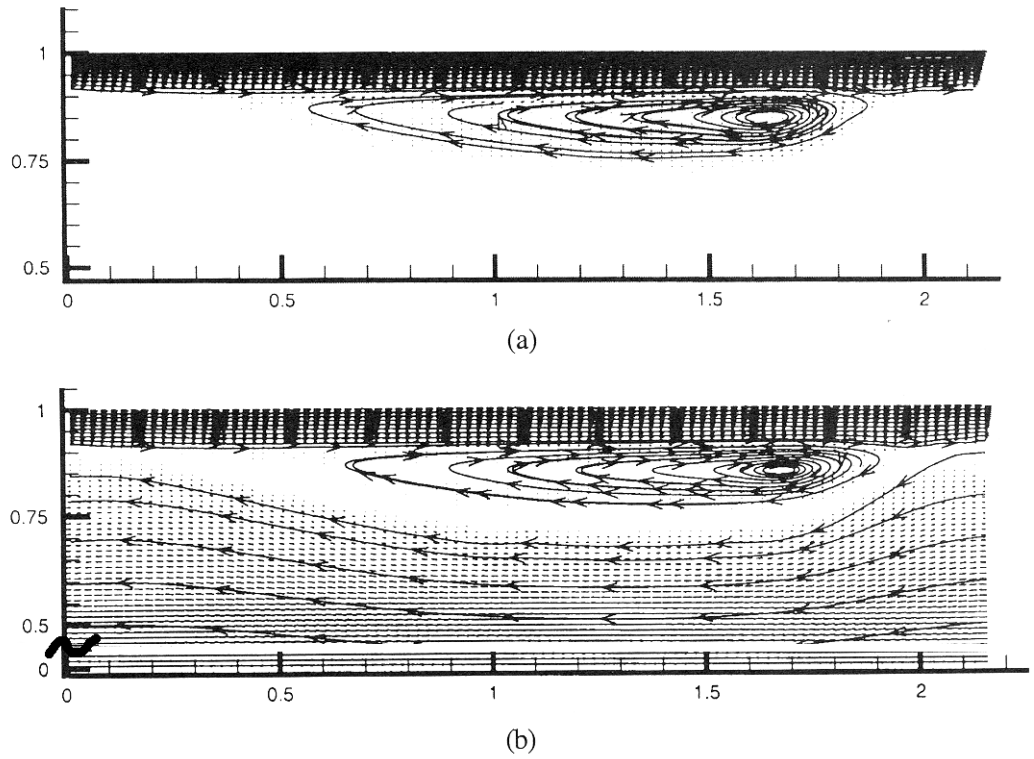

Figure 4. Streamlines and secondary motion for (a) rigid core and (b) perturbation theory when $[\eta,h,\mathbf{R},J] = [0.8, 1.4, 600, 13\times10^4]$.[20]

V Numerical simulation of wavy core flow of oil in turbulent water and turbulent gas-liquid flow with fouled pipe wall

In most pilot and test loops, and all commercial lines, the water in the annulus surrounding the oil core is turbulent and the flow in the viscous core is laminar. If the oil viscosity is very large, as is true of heavy oils and bitumen froth, secondary flows and the pressure gradients that produce them may be ignored.

Ko, Choi, Bai and Joseph[21] 2000 have developed a numerical method to predict waves on the core of viscous oil in turbulent water. The numerical code is based on the *k-*ω (shear stress transport) method proposed by Menter[22] 1994. There are no adjustable parameters in this code. Computed results using this code are in agreement with experiments. A few of these results are mentioned below (see table 1 and figure 7) and more can be found in the paper posted on our web site, *http://www.aem.umn.edu /Solid-Liquid_Flows/.*

We are proposing to use our code to study the efficiency of lubrication (the coefficient ψ in the Blasius expression (1)) in core flow of viscous oil in an annulus of turbulent water next to a fouled pipe wall, and in a turbulent gas flow in a pipe whose walls are covered by a liquid (annular gas-liquid flow).

We used Menter's shear stress transport k-ω model to solve the turbulent kinetic energy and dissipation rate equations (see Appendix B), and a four step fractional split method to solve the Navier-Stokes equations. A streamline upwind Petrov-Galerkin method is adopted for the convection dominated flow. Menter's model utilizes the original k-ω model of Wilcox in the inner region of the boundary layer and switches to the standard k-ε model in the outer region of the boundary layer.

The turbulent code was validated for the case of developing Poiseuille flow in the flow of a single fluid in a pipe at Reynolds numbers from 200 to 40,000. The length of the computational domain is sufficient to get a fully developed profile for velocity, pressure and kinetic energy. The numerical simulation reproduces the laminar friction factor $\lambda = 64/\mathrm{Re}$ and turbulent friction factor $\lambda = 0.316/\mathrm{Re}^{1/4}$ with high accuracy (figure 5) and the velocity profile in developed flow is close to the values computed by direct numerical simulation (figure 6).

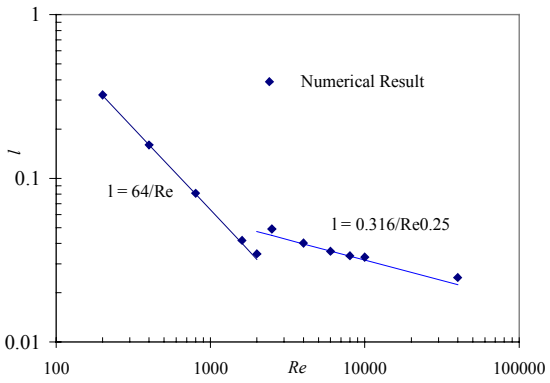

Figure 5. The friction factor vs. Reynolds number in the fully developed pipe flow.

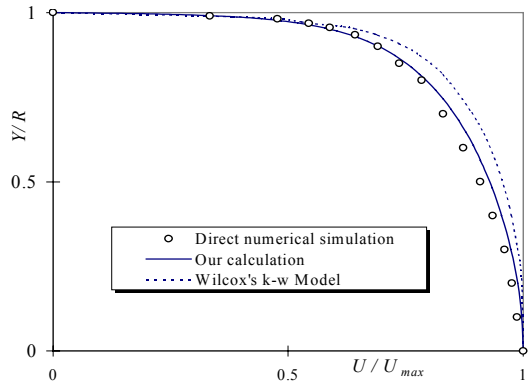

Figure 6. The velocity profile of the turbulent pipe flow at Re = 40,000.

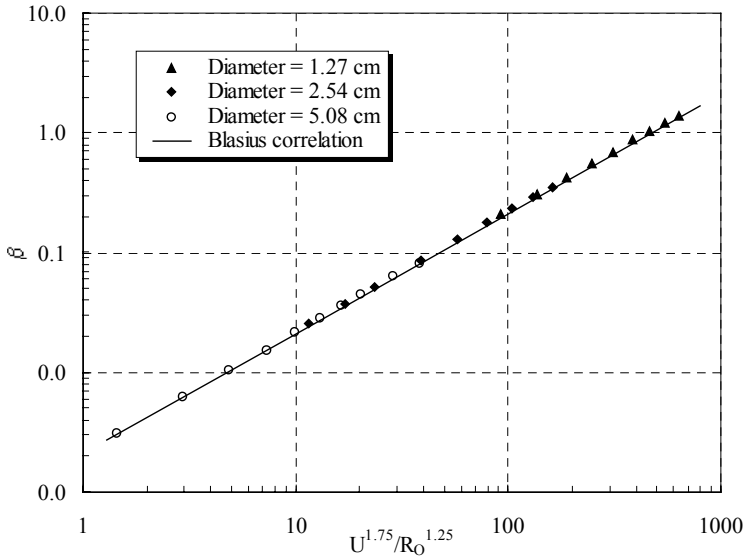

Figure 7. Pressure gradient vs. Blasius parameter $U^{1.75}/R^{1.25}$ for wavy core annular flow.

Ko *et al* 2000 applied the turbulence code to the computation of waves and friction factor on a very viscous core in which the core moves forward with a uniform motion (relative motion in the core is suppressed) but the core deforms under normal stresses from turbulent water. This kind of approximation was introduced by Bai, Kelkar and Joseph[15] 1996 for laminar flow. The effects of turbulence may be suppressed in the model by putting $k = 0$; in this case we have the "laminar" flow equations of Bai *et al* 1996. Turbulence has a very strong effect as is seen in table 1, where experiments of Bai, Chen and Joseph 1992 are compared with results from the laminar and turbulent calculations; the results computed with the turbulent code are much closer to experiments, and the error decreases as the Reynolds number increases.

The Blasius friction factor correlation (1) was also computed using the turbulent code. The code gives rise to a perfect agreement with the Blasius correlation with respect to the dependence on the velocity $U^{7/4}$ and radius $R_O^{5/4}$. The two-phase flow factor $\psi = 3.17/3.16$ for this calculation is essentially $\psi = 1$. It can be said that wavy core flow of an infinitely viscous core in turbulent water can be transported as cheaply as water alone.

Reynolds Number		4000.2	4684.6	5333.6	5811.5	8000.4
Dimensionless Wavelength (L*)	Experiments	1.35786	1.23102	1.07574	1.02346	0.82907
	Laminar Code	1.91	1.83	1.76	1.72	1.6
	Turbulent Code	1.55	1.34	1.2	1.11	0.9
Error (%)	Laminar Code	28.9078	32.7311	38.8784	40.4963	48.1828
	Turbulent Code	12.3961	8.13281	10.355	7.79613	7.88061

Table 1. The comparison of measured and computed values of wavelength at $h = 1.4$ and $\eta = 0.826$.

To explain the increase in the frictional resistance ($\psi = 10$ or 20) in the self-lubricated flow of bitumen froth evident in figure 2 we need to consider the dissipation due to the propagation of waves in the oil. Waves do not propagate on the infinitely viscous case; this is probably why $\psi = 3.17/3.16$ for this case. In the next turbulence calculation we will relax the assumption that the core is infinitely viscous (as we did in the laminar case in figure 4) and then calculate ψ. The large increase in ψ seen in figure 2 is very likely due to fouling waves develop on the fouled walls of the pipe; these are the "tiger waves" shown in figure 9. The same kind of waves occur in annular flows of turbulent gas driving liquid waves, shown in figure 10. Ultimately we are proposing to do turbulence calculations for the situations in figures 9 and 10.

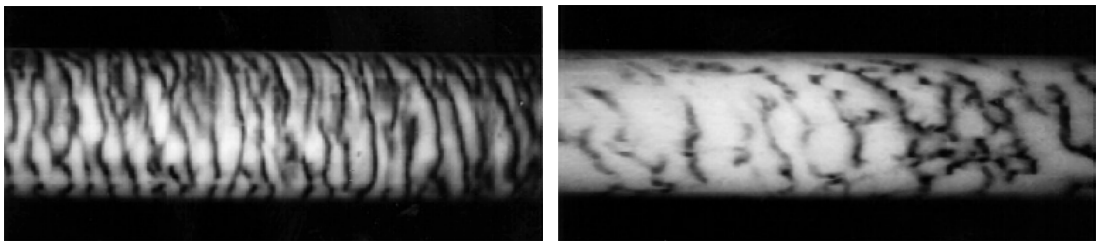

Figure 8. (Joseph, Bai, Mata, Sury, Grant 1999.) Tiger waves of bitumen froth in water with colloidal clay.

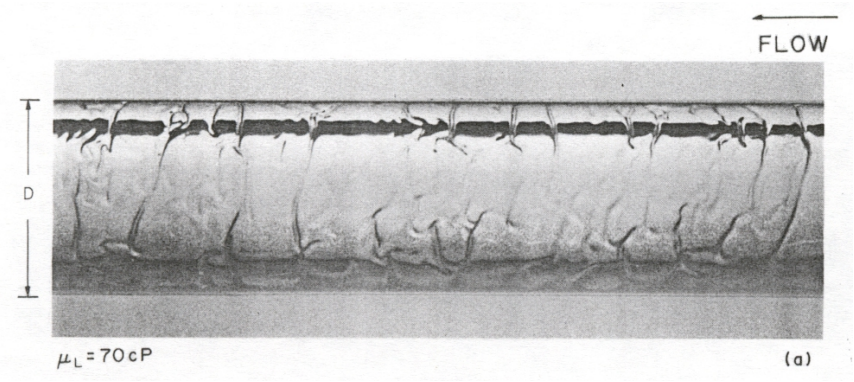

Figure 9. (Andritsos and Hanratty 1987, D = 2.52 cm.) Tiger waves on 70 cp liquid in turbulent air flow.

VI Analysis of frictional heating in turbulent two-phase flow

It is generally believed that frictional heating in the pipelining of Newtonian fluids is not important. In the Minnesota experiments on self-lubrication of bitumen froth in a one-inch pipeline, the froth temperature increased strongly with flow speed when the pipe-wall temperature was not controlled. Temperature vs. velocity for the Minnesota experiment is plotted in figure 10. The temperature rise is nearly proportional to U^2; this is consistent with frictional heating generated by a heat source of magnitude $\bar{\mu}(d\bar{u}/dy)^2$ where $\bar{\mu}$ is an effective viscosity and $d\bar{u}/dy$ an effective shear rate in a layer of sheared froth near the wall. It is instructive to think that the effective viscosity is an "eddy" and to estimate it as $\rho\langle u^{12}\rangle^{1/2}\sigma$ where $\rho = 1$ gm/cc, $\langle u^{12}\rangle^{1/2} = 5\%$ of the mean velocity and σ is the size of a large eddy. Using data given in table 4 of Joseph *et al* 1999 we have the mean as 100 cm/sec and $\sigma = 0.5$ mm; then $\hat{\mu} = 5(0.5) = 1$ poise. The eddy viscosity is 100 times the molecular viscosity of water and produces 100 times more heating. Clearly a more rigorous approach to this question should be developed.

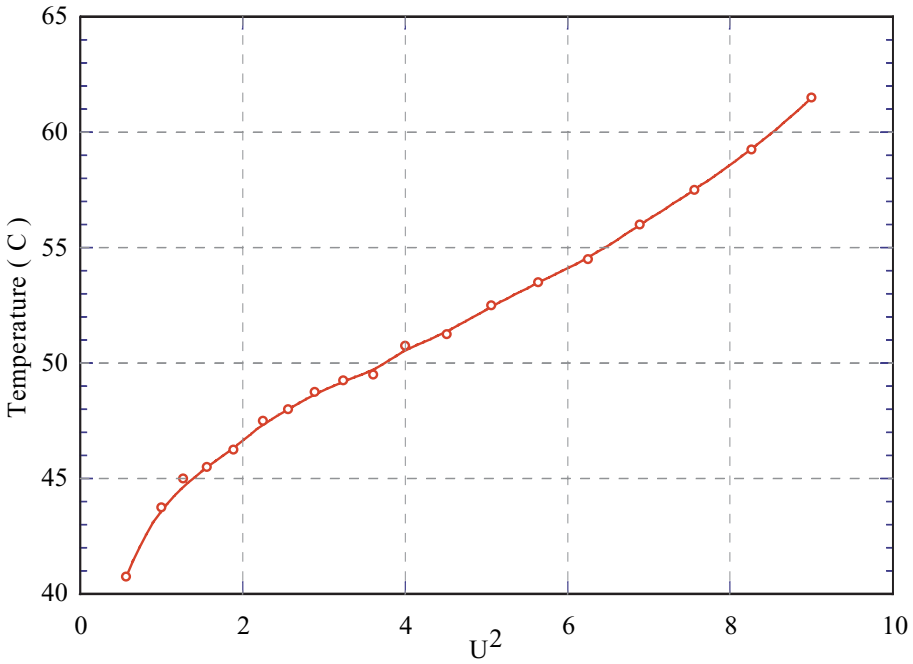

Figure 10. Temperature vs. the square of the flow speed in a 25mm diameter pipe. The temperature of the room was 26°C and the froth temperature was not controlled; the increase in temperature is due to frictional heating.

Data from Syncrude's 36" commercial pipeline does not give evidence of frictional heating. This suggests that frictional heating is a strong function of pipe diameter and that scaling laws are far from evident.

We have not found a literature on frictional heating of multiphase pipelining. We are proposing to carry out a mathematical analysis of frictional heating of core annular flow both in laminar and turbulent flow. One goal is the development of k-ω model for the temperature generated by heat dissipation in turbulent water. We would seek to predict data obtained in our one-inch pipeline and in Syncrude's 36" commercial pipeline.

The development of a working theory of frictional heating in turbulent multiphase pipelining is a challenging modeling problem whose solution could have practical applications.

VII Gas-liquid flow in pipelines

We are going to bring two new methods to the analysis of gas-liquid flows in pipelines. The simulation method we plan to use to use to analyze turbulent annular gas-liquid flows (figure 10) has already been described. The second new method makes use of a theory of viscous and viscoelastic potential flow that is discussed in section IX. This theory will be applied to the study of stability and bifurcation of stratified flow in rectangular, circular, horizontal, tilted and vertical pipelines. The third method is an application of level set methods to several variants of the Taylor bubble. Unlike the other two methods, the level set method is not our invention; we are using the method to

explain anomalous results like the independence of the rise velocity on bubble and the enhancement of the rise velocity with wetted area of inserted rods and strips.

We plan collaborative studies of gas-heavy oil flows with Intevep S.A., which is the research division of PDVSA, the Venezuelan national oil company. I have worked with this company for many years over a very wide range of projects. I have advised three Venezuelan students from INTEVEP to a PhD and one to a Masters degree. At present, I have one Masters degree student and two PhD students from Intevep. The company supports all these students; it costs them $250,000 to educate a PhD student. The quality of these students is excellent since only the best are selected for such a scholarship.

Besides working with my students on academically viable projects of interest to Intevep and oil companies, generally I do research with people from the company, at the company for weeks three times a year and remotely at other times. Three or four archival papers authored jointly with Venezuelans have appeared year after year.

For this project I propose to work on gas liquid pipeline flows with a group of about 8 persons at the company. We are going to focus on flow transitions and pressure drop formulas in cases of transport of hydrocarbons, which we have not yet a well developed understanding. New problems and approaches will be described in section III.

We have excellent experimental facilities to study gas liquid flows at Intevep that are described in appendix 2. These facilities allow me to construct real tests of our theoretical ideas.

VIII Flow charts for gas-liquid flow. Multiple solutions. Transition to annular flow.

Multiphase flow through pipes and annular ducts is an important technical subject in the oil industry. Detailed knowledge of this kind of flow is fundamental for the oil production system's proper design. Multiphase flow systems are highly complex and many aspects of its behavior are not well understood today. This lack of knowledge is especially critical in the case of heavy/extra-heavy oils. In order to design the facilities (selection of pipes, pumps, motors, etc.) traditional correlations of pressure gradient are used. These correlations were developed using fluids with viscosities ranging from 1 to 5 cP. Nevertheless, even for these low viscosity liquids, errors in pressure gradient calculations can be between 20% [23] and 30% [24]. These errors will be greater in the case of extra-heavy oils that can have up to 3000 cp.

The study of gas-heavy oil flow is best done as an emphasis in a general study of gas-liquid flow in which flow regime transitions, like the transition from stratified to slug flow are targets.

The most common correlation used to calculate the conditions for the transition from one flow regime to another is the Mandhane plot[25] shown in figure 11.

Lin and Hanratty 1987[26] note that "…the general consensus is that this plot is most reliable for air and water flowing in a small diameter pipe." They get a quite different flow chart even for air and water, when the pipe diameter is larger as shown in figure 12.

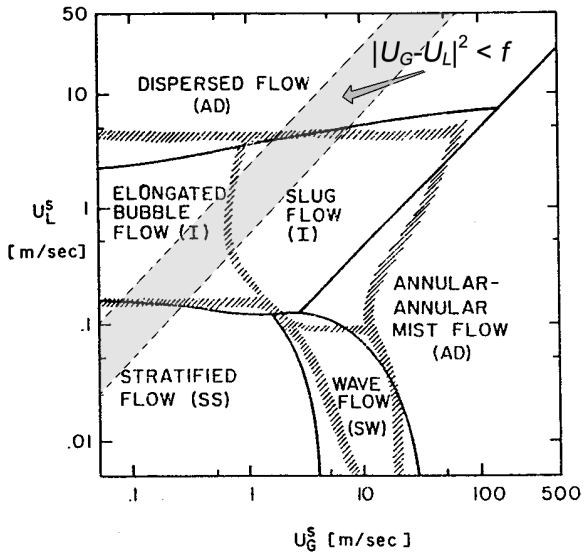

Figure 11. (After Taitel & Dukler 1976). Comparison of theory and experiment. Water-air, 25°C, 1 atm, 2.5 cm. diameter, horizontal. — theory; ///// Mandhane et al, 1974. Regime descriptions as in Mandhane.

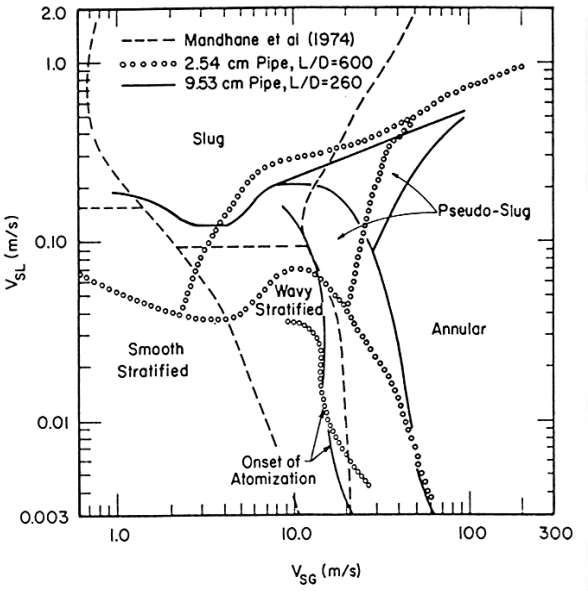

Figure 12. (After Lin & Hanratty, 1987.) Flow regime map for air and water flowing in horizontal 2.54cm and 9.53cm pipes.

The Mandhane charts cannot well describe the flow regimes that can arise in all circumstances. The coordinates of the charts are superficial velocities, dimensional quantities that do not reflect any consequence of similarity, Reynolds numbers, Weber numbers etc. Mandhane charts lack generality since each sheet requires specification of a set of relevant parameters like fluid viscosity, surface tension, pressure level and gas density, turbulence intensity data, pipe radius, gas fraction, etc.

Mandhane charts assume that flow regimes are unique and do not acknowledge the fact that nonlinear system allow multiple solutions; for example, Wallis and Dobson[27] 1973 have shown that apparently stable slug flow can be initiated by large disturbances in the region where stratified flow is stable (see their section titled "Premature slugging"). Slugs are always formed in the 2" Intevep flow loop in gas-oil (μ = 400 cp) flows at even the smallest velocities that can be achieved in the system. These slugs are separated regions of apparently stable stratified flow with a perfectly flat free surface. The length of stable stratified flow between slugs can be nearly the length of the flow loop. This may also be interpreted as "premature" slugging though it is more appropriate to describe it as a multiple solution; slug flow and stratified flow exist at one and the same point on the flow chart.

From the practical point of view the existence of multiple solutions point to the desirability of a careful analysis of domains of attraction of stable solutions. The appearance of slugs in a region of stable stratified flow points to a careful analysis of the disturbance level at the inlet where large waves may be created. At the end of the paper on waves Crowley, Wallis and Barry[28] 1992 write that

> When a new slug forms it requires additional pressure drop to accelerate it. This feeds back to the inlet by acoustic waves in the gas (which can travel upstream) and changes the conditions there. This new "disturbance" eventually grows to form a slug and the cycle repeats. The method of characteristics can represent this cycle, but assumptions (or a separate mechanistic analysis) are needed about this inlet behavior.

It is at present not possible to predict the transition of one flow type to another. The dependence of the empirical charting of flows is also incomplete; there is only sparse data on the dependence of flow type on pipe radius, liquid viscosity, pressure level, atomization level, turbulent intensity. Pressure gradients vs. volume flux, holdup of phases and other process control data are not predictable from first principles or from empirical flow charting.

We propose to study the transition of stratified flow to wavy flow and the transition to annular flow in hydrocarbon systems with viscosities greater than 100 cp. We are going to analyze the effect of turbulence on the flow charts in general and for the targeted systems; we will use our k-ω model and experimental data to determine the increases in the pressure drop in annular flow due to liquid on the wall and atomization over the pressure drop for turbulent gas flow for dry gas in a clean pipe. This increase will be expressed in terms of the friction factor efficiency factor ψ defined in equation (1).

We are also looking at y by processing the huge database in the literature. Our studies have already suggested that increases in friction correlate with the amount of liquid on the wall, with liquid holdup. Wave propagation in a deep liquid layer might increase friction. Unfortunately, holdup data is not usually given in published data.

IX Viscous potential flow (VPH) analysis of Kelvin-Helmholz instability in rectangular conduits

It is well known that the Navier-Stokes equations are satisfied by potential flow; the viscous term is identically zero when the vorticity is zero but the viscous stresses are not zero (Joseph and Liao[29] 1994). It is not possible to satisfy the no-slip condition at a solid boundary or the continuity of the tangential component of velocity and shear stress at a fluid-fluid boundary when the velocity is given by a potential. The viscous stresses enter into the viscous potential flow analysis of free surface problems through the normal stress balance at the interface. Viscous potential flow analysis gives good approximations to fully viscous flows in cases where the shears from the gas flow are negligible; the Rayleigh-Plesset bubble is a potential flow which satisfies the Navier-Stokes equations and all the interface conditions. Joseph, Belanger and Beavers[30] 1999 constructed a

viscous potential flow analysis of the Rayleigh-Taylor instability that can scarcely be distinguished from the exact fully viscous analysis.

The success of viscous potential flow in the analysis of Rayleigh-Taylor instability has motivated the analysis of Kelvin-Helmholz (KH) theory given in the recent short paper by Joseph, Lundgren and Funada[31] 2000 and in a very detailed viscous potential flow analysis of KH instability in a rectangular duct by Funada and Joseph[32] 2000. As we have already mentioned potential flow requires that we neglect the no-slip condition at solid surfaces. In the rectangular channel the top and bottom walls are perpendicular to gravity; the bottom wall is under the liquid and parallel to the undisturbed uniform stream; the top wall contacts gas only. The side walls are totally inactive; there is no motion perpendicular to the side walls unless it is created initially and since the two fluids slip at the walls all the conditions required in the analysis of three dimensions can be satisfied by flow in two dimensions.

The viscosity in viscous potential flow enters into the normal stress balance rather than tangential stress balance. Air over water induces small viscous stresses that may be confined to boundary layer and may be less and less important as the viscosity of the liquid increases. At a flat, free surface $z = 0$ with velocity components (u,w) corresponding to (x,z) the shear stress is given by

$$\mu\left(\frac{\partial u}{\partial z}+\frac{\partial w}{\partial x}\right) \qquad \text{and the normal stress is} \qquad 2\mu\frac{\partial w}{\partial z}$$

The normal stress is an extensional rather than a shear stress and it is activated by waves on the liquid; the waves are induced more by pressure than by shear. For this reason, we could argue that the neglect of shear could be justified in wave motions in which the viscous resistance to wave motion is not negligible; this is the situation which may be well approximated by viscous potential flow.

The prescription of a discontinuity in velocity across $z = 0$ is not compatible with the no-slip condition of Navier-Stokes viscous fluid mechanics. The discontinuous prescription of data in the study of KH instability is a viscous potential flow solution of the Navier-Stokes in which no-slip conditions at walls and no slip and continuity of shear stress across the gas liquid surface are neglected. Usually the analysis of KH instability is done using potential flow for an inviscid fluid but this procedure leaves out certain effects of viscosity that can be included with complete rigor. This kind of analysis using viscous potential flow has been constructed by Funada and Joseph 2000.

For 2D disturbances of stratified flow the disturbance potential is given by

$$\phi = A \pm e^{\sigma t} e^{ikx} \cosh k(z \quad h\pm) \tag{1}$$

where $\partial\phi/\partial z = 0$ at the top and bottom wall, k is the wave number and σ is an eigenvalue $\sigma = \sigma_R + i\sigma_{\text{i}}$ and σ_R is the growth rate. The dispersion relation for σ is found in the form

$$\begin{aligned}&\left[\rho_a(\sigma+ikU_a)^2+2\mu_a k^2(\sigma+ikU_a)\right]\coth(kh_a)\\&+\left[\rho_l(\sigma+ikU_l)^2+2\mu_l k^2(\sigma+ikU_l)\right]\coth(kh_l)+(\rho_l-\rho_a)gk+\gamma k^3=0\end{aligned}\tag{2}$$

where the subscript *a* stands for air and *l* for liquid.

The neutral curve $\sigma_R(k) = 0$ gives the border between stability and instability. This neutral curve can be expressed in dimensionless form as

$$\hat{V}=\frac{\left[\tanh\left(\hat{k}\,\hat{h}_a\right)+\hat{\mu}\tanh\left(\hat{k}\,\hat{h}_l\right)\right]^2}{\tanh\left(\hat{k}\,\hat{h}_a\right)+\left(\hat{\mu}^2/\hat{\rho}\right)\tanh\left(\hat{k}\,\hat{h}_l\right)}\frac{1}{k}\left[1+\frac{\hat{\gamma}\hat{k}^2}{(1-\hat{\rho})}\right]\tag{3}$$

where

$$\hat{V}^2\equiv\left(\hat{U}_a-\hat{U}_l\right)^2,\tag{4}$$

$\hat{\gamma}$ is surface tension and

$$\hat{\mu}=\frac{\mu_a}{\mu_l},\ \hat{\rho}=\frac{\rho_a}{\rho_l}.\tag{5}$$

The stability criterion is symmetric with respect to $\hat{U}_a$ and $\hat{U}_l$. Because the problem is Galilean invariant the flow seen by the observer moving with gas is the same as the one seen by an observer moving with the liquid. Nearly all authors who study KH instability get a criterion of stability like (3) with stability when

$$\hat{V}^2<f\tag{6}$$

with different *f* dependent on the author. This criterion is plotted in figure 11; it is not consistent with many flow charts. When $\hat{\mu}=\hat{\rho}$ equation (3) reduces to the neutral curve for an inviscid fluid. It can be shown that for each fixed $\hat{k}$, $\hat{V}^2$ is maximum when $\hat{\mu}=\hat{\rho}$. All viscous fluids with $\hat{\mu}\neq\hat{\rho}$ have a lower stability limit; hence the stability for an inviscid fluid is maximum among all viscous fluids.

The gas fraction is $\hat{h}_a=\alpha$ and since $\hat{h}_l=1-\alpha$, (3) is determined by α, the ratios (5), $\hat{\gamma}$ and the wave number $\hat{k}$. The stability limit is then obtained as

$$\hat{V}^2_{\min}=\min_{\hat{k}}\hat{V}^2(\hat{k})\tag{7}$$

The heavy black line in figure 13 is the stability limit from viscous potential flow; it corresponds to the minimum value of $\hat{V}^2$ over $\hat{k}$ of different gas fractions α. The effects of surface tension are always important and actually determine the stability limits for the cases in which the volume fraction is not too small.

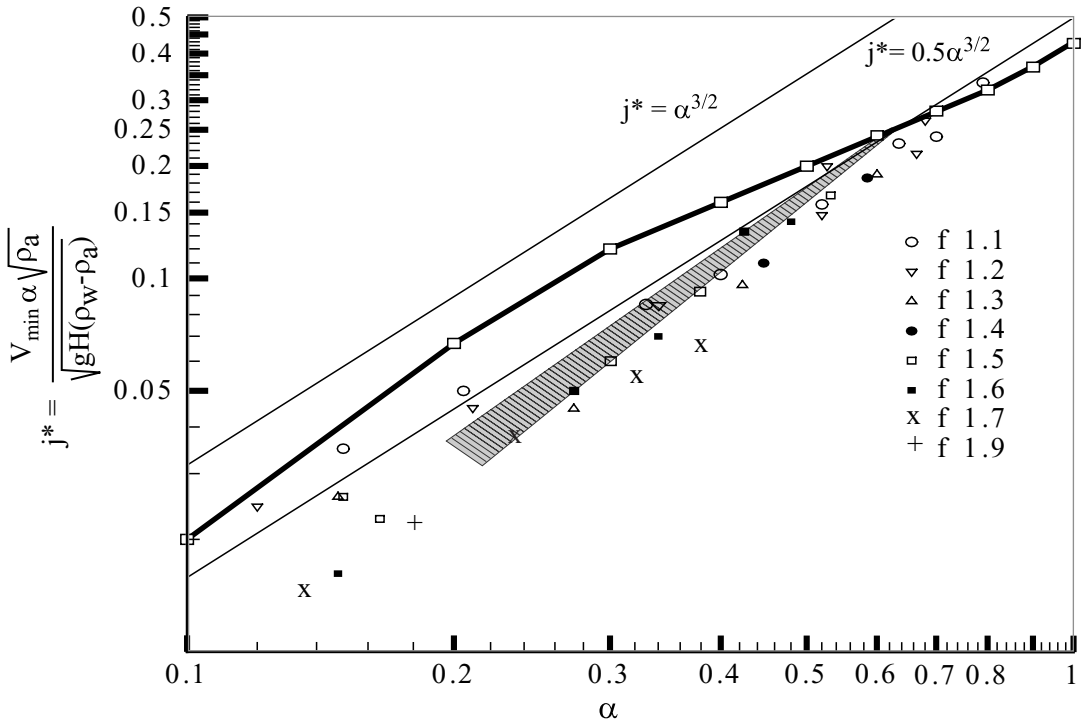

Figure 13. j^* vs. α. Comparison of theory and experiments. $j^* = \alpha^{3/2}$ is the long wave criterion for an inviscid fluid put forward by Wallis and Dobson 1973. $j^* = 0.5\ \alpha^{3/2}$ was proposed by them as best fit to the experiments f 1.1 through f 1.9 described in their paper. The shaded region is from experiments by Kordyban and Ranov 1970.

The interpretation of the results shown in figure 13 is not straightforward; on a superficial level it can be said that the criterion for stability of stratified flow given by viscous potential flow is in good agreement with experiments when the liquid layer is thin, but it over predicts the data when the liquid layer is thick.

The most interesting aspect of our potential flow analysis is the surprising importance of the viscosity ratio $\hat{\mu} = \mu_a / \mu_l$ and density ratio $\hat{\rho} = \rho_a / \rho_l$; when $\hat{\mu} = \hat{\rho}$ the equation (3) for marginal stability is identical to the equation for the neutral stability of an inviscid fluid even though $\hat{\mu} = \hat{\rho}$ in no way implies that the fluids are inviscid. Moreover, the critical velocity is a maximum at $\hat{\mu} = \hat{\rho}$; hence the critical velocity is smaller for *all* viscous fluids such that $\hat{\mu} \neq \hat{\rho}$ and is smaller than the critical velocity for inviscid fluids. All this may be understood by inspection of figure 13, which shows that $\hat{\mu} = \hat{\rho}$ is a distinguished value that can be said to divide high viscosity liquids with $\hat{\mu} < \hat{\rho}$ from low viscosity liquids. As a practical matter the stability limit of high viscosity liquids can hardly be distinguished from each other while the critical velocity decreases sharply for low viscosity fluids.

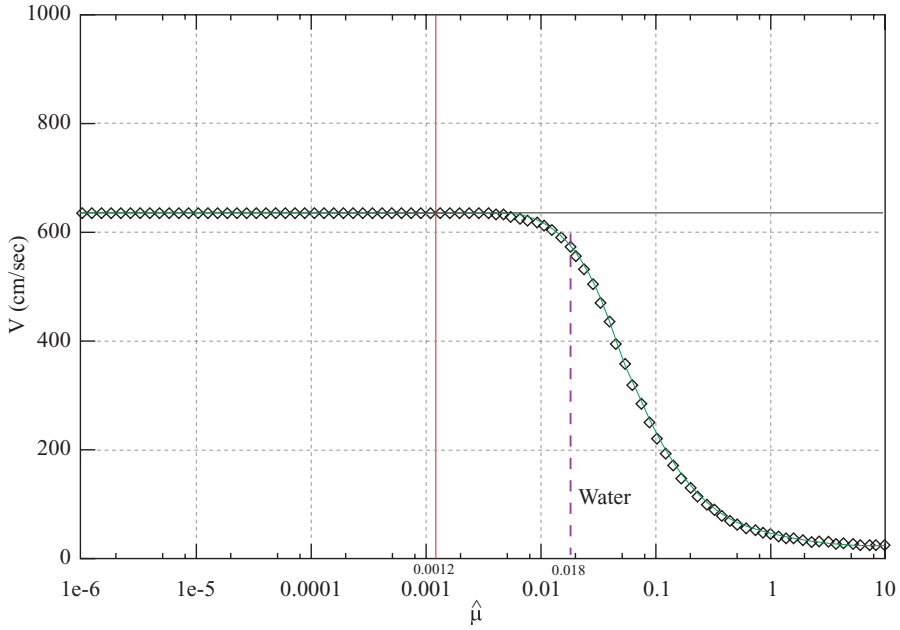

Figure 14. Critical velocity $\hat{V}=|U_a - U_l|$ vs. $\hat{\mu}$ for $\alpha = 0.5$. The critical velocity is the minimum value on the neutral curve. The vertical line is $\hat{\mu} = \hat{\rho} = 0.0012$ and the horizontal line at $\hat{V} = 635.9$ is the critical value for inviscid fluids. The vertical dashed line at $\hat{\mu} = 0.018$ is for air and water.

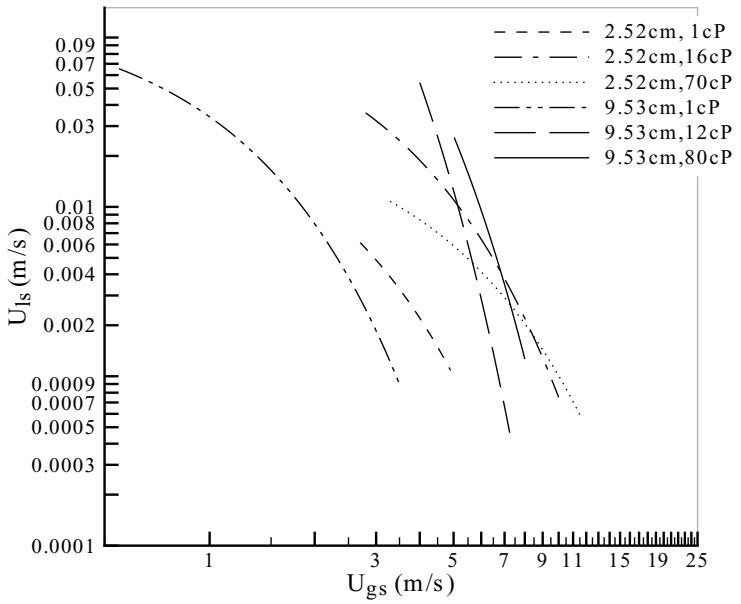

Figure 15. (After Andritsos and Hanratty 1987.) These lines represent the borders between smooth stratified flow and disturbed flow observed in experiment. The water-air data is well below the cluster of high viscosity data that is bunched together. U_{ls} is a superficial velocity.

The condition $\hat{\mu} = \hat{\rho}$ can be written as

$$\mu_l = \mu_a \frac{\rho_l}{\rho_a} . \tag{8}$$

For air and water

$$\mu_l = 0.15 \text{ poise} . \tag{9}$$

Hence $\mu_l > 0.15$ poise is a high viscosity liquid and $\mu_l < 0.15$ poise is a low viscosity liquid provided that $\rho_l \approx 1$ gm/cm^3.

Other authors have noted strange relations between viscous and inviscid fluids. Barnea and Taitel[33] 1993 note that "the neutral stability lines obtained from the viscous Kelvin-Helmholtz analysis and the inviscid analysis are quite different for the case of low liquid viscosities, whereas they are quite similar for high viscosity, contrary to what one would expect." Their analysis starts from a two-fluid model and it leads to different dispersion relations; they do not obtain the critical condition $\hat{\mu} = \hat{\rho}$. Earlier, Andritsos, Williams and Hanratty[34] 1989 noted a "surprising result that the inviscid theory becomes more accurate as the liquid viscosity increases."

Andritsos and Hanratty[35] 1987 have presented flow regime maps for pipe flows in 2.52cm and 9.53cm pipe for fluids of different viscosity ranging from 1 cp to 80 cp. These figures present flow boundaries; the boundaries of interest to us are those that separate "smooth" flow from disturbed flow. Liquid holdups (essentially α) are not specified in these experiments. We extracted the smooth flow boundaries from figures in Andritsos & Hanratty and collected them in our figure 14. It appears from this figure that the boundaries of smooth flow for all the liquids with $\mu_l > 15$ cp are close together, but the boundary for water with $\mu_l = 1$ cp is much lower.

New research projects

(1) There is great interest in the oil industry in tilted pipes, say going uphill and downhill.

Do a viscous potential flow analysis of the stability of stratified flow in slightly tilted from horizontal rectangular conduits.

(2) A Sharki and T. Hanratty[36] 2000 have recently demonstrated that polymer additives reduce drag dramatically in turbulent gas-liquid annular flows in pipes. Even more memorable is that the effect these highly diluted solutions have on the free surface; the flow type changes to stratified with small waves. The effects of additives on gas-liquid flows was reviewed by Manfield, Lawrence and Hewitt[37] 1999.

Construct a viscoelastic potential flow analysis of the stability of stratified flow of viscoelastic (Oldroyd B) fluids in horizontal rectangular conduits. We have already constructed an analysis Rayleigh-Taylor stability of viscoelastic drops in high-speed air

streams at ultra high Weber numbers. We used an Oldroyd B model. The analysis can be fit to the observations by the selection on very small retardation times.

There is controversy about drag reduction in dilute polymer solutions and perhaps the majority think it can't be explained by Oldroyd B models. However our very accurate calculations do give rise to drag reductions matching experiment (Min, Yoo, Choi and Joseph[38] 2000).

(3) There is no analysis of stability in round pipes that respect the geometry of the pipe by enforcing the condition that the pipe wall is a streamline. This is a difficult problem that is much simpler but still difficult in the context of viscous potential flow in which the potential ϕ satisfies Laplace's equations. If x is the axis and r, θ are polar coordinates in the cross section, we look for eigenfunctions

$$\phi(r,\theta,x,t) = e^{\sigma t}e^{ikx}\Phi(r,\phi,k)$$

such that

$$\frac{\partial \Phi}{\partial r}(a,\theta,k) = 0$$

where $r = a$ is the pipe wall. *The determination of representations of the functions Φ above and below the flat free surface at y = 0 is not straightforward and is the main obstacle to be overcome.*

X Nonlinear effects. Bifurcation analysis of KH instability using viscous potential flow. Multiple solutions.

There is no theory that is faithful to all conditions at play in experiments. None of the theories agree with experiments. Attempts to represent the effects of viscosity are only partial, as in our theory of viscous potential flow, or they require empirical data on wall and interfacial friction, which are not known exactly and may be adjusted to fit the data. Some choices for empirical inputs underpredict and others overpredict the experimental data.

It is widely acknowledged that nonlinear effects at play in the transition from stratified to slug flow are not well understood. The well-known criteria of Taitel and Dukler[39] 1976, based on a heuristic adjustment of the linear inviscid long wave theory for nonlinear effects, is possibly the most accurate predictor of experiments. Their criterion replaces $j^* = \alpha^{3/2}$ with $j^* = \alpha^{5/2}$. We can obtain the same heuristic adjustment for nonlinear effects on viscous potential flow by multiplying the critical value of velocity in figure 13 by α. Plots of $j^* = \alpha^{3/2}$, $j^* = \alpha^{5/2}$ and the heuristic adjustment of viscous potential flow, together with the experimental values of Wallis and Dobson[24] 1973, and Kordyban and Ranov[40] 1970 are shown in figure 16. The good agreements in evidence there lacks a convincing foundation.

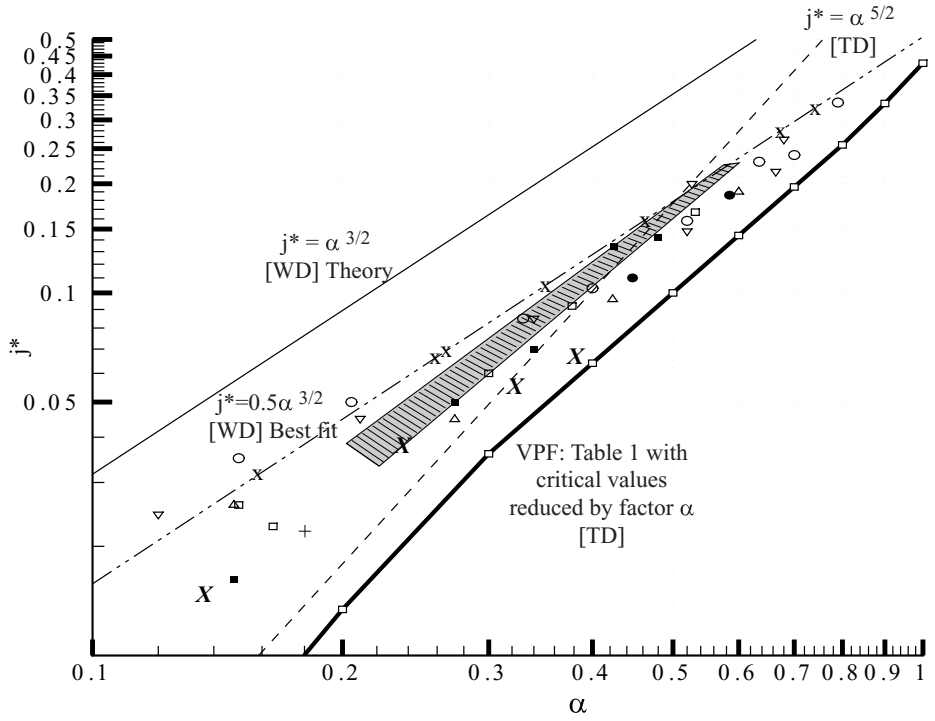

Figure 16. Nonlinear effects. The Taitel-Dukler [TD] 1976 correction (multiply by α). [WD]: Wallis and Dobson 1973.

Rigorous analytical approaches to nonlinear effects are often framed in terms of bifurcation theory. To do bifurcation analysis it is necessary to have an accurate description of the flow that bifurcates. Bifurcation analyses of stratified laminar Poiseuille flow of two liquids in channels can be found in the literature but these flows are rather different than the plug flows considered here; they satisfy no-slip conditions at all boundaries and stress continuity conditions at the interfaces. As far as I know this kind of analysis has not been applied to gas-liquid flows possibly because the gas is turbulent even over much of the region where stratified flow is stable.

One value of bifurcation theory is that many of its results are generic so that aspects of nonlinear behavior apply to many different kinds of problems without knowing details of any one. In the usual case the bifurcation of the basic flow occurs at a critical point; in the case of KH instability we lose stability of plug flow when $\hat{V}$ exceeds the critical value $\hat{V}_c$, which for VPF are the points on the heavy line in figure 13. For $\hat{V} > \hat{V}_c$ the basic flow is unstable. Generically a nonlinear solution will bifurcate at criticality; if the nonlinear solution bifurcates with $\hat{V} > \hat{V}_c$ it is supercritical and generically stable, if $\hat{V} < \hat{V}_c$ it is subcritical and generically unstable. In the case of KH instability the basic solution is unstable to a time periodic disturbance so that the bifurcating solutions will also be time periodic; this is called a Hopf bifurcation (see Iooss and Joseph[41] 1990).

At criticality, the time periodic solution has a characteristic frequency $\omega = c\hat{k}$ where c is a wave speed and $\hat{k}$ a wave number. A bifurcation time periodic solution can be determined only up to a change of phase. The amplitude ε of the wave can be regarded in

the bifurcation parameter; it can be positive or negative and is conveniently described by projections on the null spaces of the adjoint operator (Iooss and Joseph, Chapter VII).

We may formulate the bifurcation analysis in a frame moving with water; the $\hat{V} = U$ is the velocity of air. We seek a bifurcating solution $U(\varepsilon)$ with a frequency $\omega(\varepsilon)$ obtained by scaling time $\partial / \partial \hat{t} = \omega \partial / \partial t$ and write the governing equations for viscous potential flow with potential $\hat{\phi}$ as follows:

$$\nabla \hat{\phi} = U + \varepsilon \nabla \phi, \quad \mathbf{U} = \mathbf{e}_x U, \quad \nabla^2 \phi = 0$$

It is understood that each equation must be written twice, for the gas with parameters (U, μ_g, ρ_g) and the liquid (0, μ_l, ρ_l).

$$\rho \left[\omega \frac{\partial \nabla \phi}{\partial t} + U \frac{\partial \phi}{\partial x} + \frac{\varepsilon}{2} \nabla \left(\nabla \phi^2 \right) \right] = -\nabla p$$

On the interface $z = h(x,y,t)$ we have

$$\frac{\partial \phi}{\partial z} = \omega \frac{\partial h}{\partial t} + U \frac{\partial h}{\partial x} + \varepsilon \left[\frac{\partial \phi}{\partial x} \frac{\partial h}{\partial x} + \frac{\partial \phi}{\partial y} \frac{\partial h}{\partial y} \right]$$

and

$$\left[\left[-p + 4\mu n_2 \cdot \frac{\partial^2 \phi}{\partial x_i \cdot \partial x_j \cdot} n_j \right] \right] + [[\rho]] g h = -\gamma 2H$$

where H is twice the mean curvature and, for example

$$[[\rho]] = \rho_g - \rho_l$$

We seek a solution as a power series in ε. It can be shown the $U(\varepsilon)$ and $\omega(\varepsilon)$ are even functions (Iooss & Joseph, Chapter III). It follows that periodic solutions that bifurcate to one or the other side of criticality, as in figure 18, and never to both sides; periodic bifurcating solutions cannot undergo two-sided bifurcation.

It is of interest to speculate how some outstanding experimental observations on the loss of stability of stratified flow may be explained by bifurcation. First, we recall that Wallis and Dobson 1973 reported very robust data on premature slugging, slugs when $\hat{V} < \hat{V}_c$. Andritsos and Hanratty 1987 report that stratified flow loses stability to regular waves when the viscosity is small, and directly to slugs when the viscosity is large. Premature waves would be described by subcritical bifurcation as in the diagram of figure 17. A supercritical fabrication to regular waves is shown in figure 18. Perhaps there is a change from supercritical to subcritical bifurcation as the viscosity is increased in the experiments of Andritsos and Hanratty. Many other bifurcation scenarios are possible.

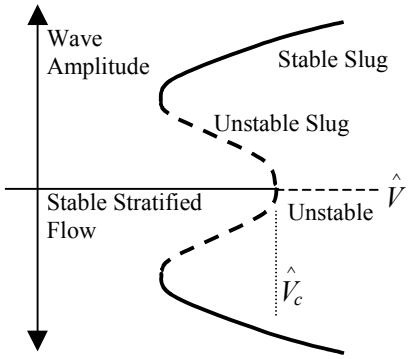

Figure 17. A speculative diagram of subcritical bifurcation to explain premature slugging.

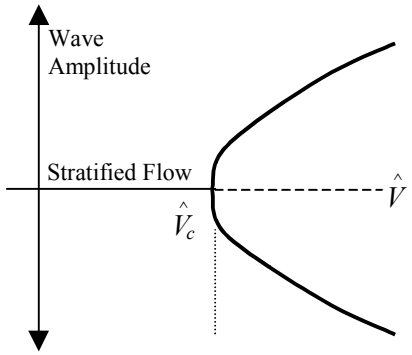

Figure 18. A speculative diagram of subcritical bifurcation to explain the supercritical bifurcation of regular waves.

XI Rise velocity of long gas bubbles in pipes and conduits

We propose to do studies to explain many unexplained and even paradoxical results for long gas bubbles, called slugs, rising in liquids in vertical pipes and conduits. Such bubbles form when the gas input is large. These kinds of bubbles can arise naturally by coalescence of small bubbles following in the wake of large gas bubbles. The formation of slugs in vertical pipelines is an important feature in the extraction of oil from a vertical well bore. The pressure depletion along the pipe will cause dissolved gases like methane and carbon dioxide to come out of solution and join the already existing gas phase.

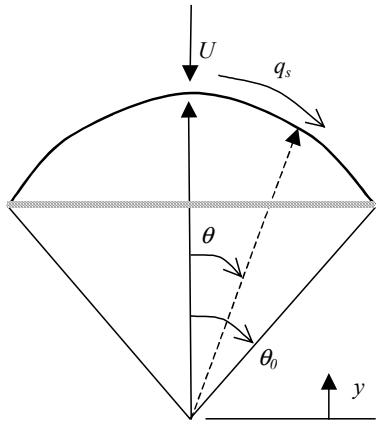

Figure 19. Spherical cap bubble

The properties of slugs, even in still liquids, which is the easiest, are really amazing. First of all, the rise velocity of the bubble can be predicted without any dynamic force balance, from the shape of the bubble alone. Secondly, the rise velocity is independent of the length of the bubble so that the usual idea based on Archidmedes principle seems not to apply here. The rise velocity of the Taylor-Davies[42] bubble and the spherical cap bubble, which was also analyzed by them, is determined by the shape of the bubble. When the radius R = D/2 of the bubble is not too small surface tension may be neglected and the pressure in the gas and on the spherical cap is constant. The Bernoulli equation on the cap is given by $-q_s^2/2 = g[R - r(\theta)\cos\theta]$. For potential flow over a sphere $q_s^2 = \frac{3}{2}U\sin\theta$. Looking near the stagnation point with $r(\theta) = R$, $\sin\theta = \theta$, $\cos\theta = 1-\theta^2/2$ they find

$$U = K\sqrt{gD}, \quad K = \frac{\sqrt{2}}{3} \tag{10}$$

where K is a shape factor. Batchelor notes that

> the remarkable feature of [equations like (10)] and its various extensions is that the speed of movement of the bubble is derived in terms of the bubble shape, without any need for consideration of the mechanism of the retarding force which balances the effect of the buoyancy force on a bubble in steady motion. That retarding force is evidently independent of Reynolds number, and the rate of dissipation of mechanical energy is independent of viscosity, implying that stresses due to turbulent transfer of momentum are controlling the flow pattern in the wake of the bubble[43].

The rise of a Taylor bubble is similar, but slightly lower, with an empirical of K about 0.35. The formula (10) for the rise velocity is independent of the length of the bubble, it is independent of the gas or liquid density or viscosity.

Another paradoxical property is that the Taylor bubble rise velocity does not depend on how the gas is introduced. In the Taylor-Davies experiments the bubble column is open to the gas. In other experiments the gas is injected into a column whose bottom is closed.

There are many studies of the effects of liquid of viscosity μ, pipe diameter, density ρ, and surface tension on the rise velocity of Taylor bubbles. Correlations by White and Beardmore[44] 1962, and Brown[45] 1965, who gives

$$U = 0.35\sqrt{gD}\left\{1 - \frac{(1+ND)^{1/2} - 1}{ND/2}\right\}^{1/2} \tag{11}$$

where

$$N = \left[14.5\frac{\rho^2 g}{\mu^2}\right]^{1/3}.$$

Equation (11) gives accurate results when $ND > 120$ and it reduces to (10) when the last term in (11) is much less than 1.

Why doesn't the rise velocity depend on the length of the Taylor bubble? If a Taylor bubble rises in steady flow it must be in a balance between buoyant weight and drag. We don't know how to compute either. If we think of Achimedes principle we would be led to think that the buoyant would increase with volume accordingly $(\rho_l - \rho_g)g$. Volume and the bubble would rise faster, just as large spherical bubbles rise faster than small one. Archimedes principle requires that the pressure of the hydrostatic impress itself on the bubble. Evidently this does not occur in the Taylor bubble.

The liquid at the wall drains under gravity without changing the pressure. The equation is

$$\mu \frac{\partial^2 U}{\partial x^2} = \rho_l g \qquad \left(\text{no } \frac{dp}{dx} \right) \tag{12}$$

Then the cylindrical part of the long bubble is effectively not displacing liquid (doesn't change pressure). The buoyancy is still the volume of the hemisphere poking into the liquid at the top. The equation of motion *buoyancy = drag* doesn't change.

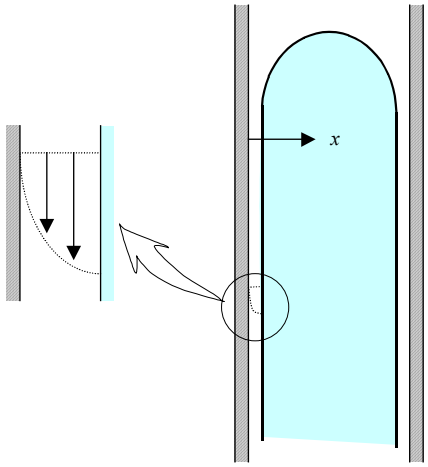

Figure 20. Drainage at the wall of a rising Taylor bubble. If -U *is added to this system the wall moves and the bubble is stationary.*

Rise velocity in annular pipes. Another paradoxical result is that if a Taylor bubble rises in the annular space between two cylinders, it will rise faster than it would if the inner cylinder were absent. Caetano, Shoham and Brill[46] 1992 studied the rise of gas bubbles in annular pipes; they note that

> For any combination of fluid pairs and annuli configurations., the Taylor bubble rise velocity is larger than predicted for a circular pipe with a diameter equal to the annulus shroud diameter. As in the circular pipe case, once the bubble cap is developed, the bubble rise velocity is insensitive to the bubble length and/or volume.

Moreover, if the perimeter of the annular increased while the radius of the outer cylinder is fixed, so that the gap between the cylinders decreases, the Taylor bubble will rise still faster. Radar, Bourgoyne and Ward[47] 1975 did experiments in a small scale apparatus and in a 6000 ft. deep well. They used water, water-glycerin and non-Newtonian fluids and air, methane and penthane as gas. They say (pg. 574) "…It was surprising that, at first, the gas bubble rose faster when the inner tube was present… More surprising was that the bubble rose even faster when the annular cross-sectional area was further reduced by increasing the diameter of the inner tube."

Bubble rise with insertions. Bubble rise velocities in configurations with and without insertions were studied by Grace and Harrison[48] (1967). They studied bubbles of Taylor type, but smaller ones, big enough to have an ellipsoidal shape but not so big as to display Taylor bubble behavior. Their basic experimental configuration was a vertical duct with a rectangular cross-sectional area. The insertions consisted of single or multiple rods, flat plates and rectangular cross section area ducts. They found that a bubble

changes its shape from a circular-cap to an elliptical-cap and, in the limit, to a parabolic-cap shape. These new shapes are a function of the particular surface inserted, and provide faster rising velocities as compared to flow without insertions.

Research questions. We are interested in Taylor bubbles and especially when they rise in oils of high viscosity. Brown 1965 and White and Beardmore[49] 1962 have shown that in certain circumstances Taylor bubbles in high viscosity liquids, as high as 450 cp will rise at the speed $0.35\sqrt{gD}$ of gas bubbles in water. The questions asked below are meant to be qualified by a specification of parameters for which they are appropriate.

- When and why is the rise velocity of the Taylor bubble independent of volume?
- When and why is the rise velocity of the Taylor bubble the same whether the bottom of the column is open or closed?
- How is bubble shape connected with wall drainage?
- How does the bubble rise velocity change with the gap size in the annulus and with drainage area on both cylinder walls?
- What is the mechanism by which inserts increase the rise velocity of Taylor bubbles?
- Is there an optimal position, type and placement of inserts for the fastest rise of Taylor bubbles in a tube with inserts?
- What is the force balance that controls the rise velocity of a Taylor bubble?
- What is the effect on all the above questions and the dynamics of Taylor bubbles generally of upflow and downflow of the liquid?

Experiments indicate that Taylor bubbles in concentric annuli are unstable. Observed gas bubbles only partially fill the annulus[45,46].

- To what extent are nonaxisymmetric shapes of bubbles stable and unique in perfectly concentric annuli?
- Compare the rise velocity of axisymmetric and nonaxisymmetric bubbles in annuli.

Research projects

The projects we propose are motivated by the research questions posed above. We plan to attack these projects with experiments and numerical simulations.

Experiments: In the Minnesota lab we will do experiments on the effects of inserts on Taylor bubbles in water. A diagram of this kind is shown below as figure 21. We will also consider the case in which the flat plate extends to the bottom of the bubble column.

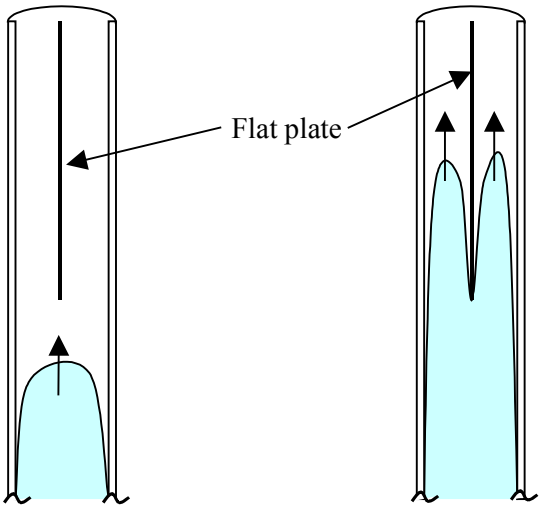

Figure 21. Diagram of the effect of a splitter plate on the rise velocity of a Taylor bubble.

The effects of upflow and downflow of water on the rise velocity of Taylor bubbles will be studied in the apparatus described in figure A.1.

Experiments of a similar type, using oils, will be carried out in Venezuela, using their excellent apparatus shown in figure A.3.

Numerical simulation

Numerical studies of Taylor bubbles rising through stagnant liquids have been given by Mao and Dukler[50] 1990 and by Bugg, Mack and Rezkallah[51] 1998. The Bugg *et al* paper covers a wider range of conditions and makes no *a priori* assumption about the shape of the leading edge or the terminal speed. They use a volume of fluid method and do extensive calculations for different values of the Froude Eötvös and Morton numbers. They obtain some reasonable agreement with experiments in the literature. They do not address the research questions posed in the previous section and they neglect surface tension.

The simulation project being proposed here is based on level set method based on a fully resolved Navier Stokes solver with no approximations developed by P. Singh 1999, 2000. This code has been programmed and preliminary results are shown in figures 22.

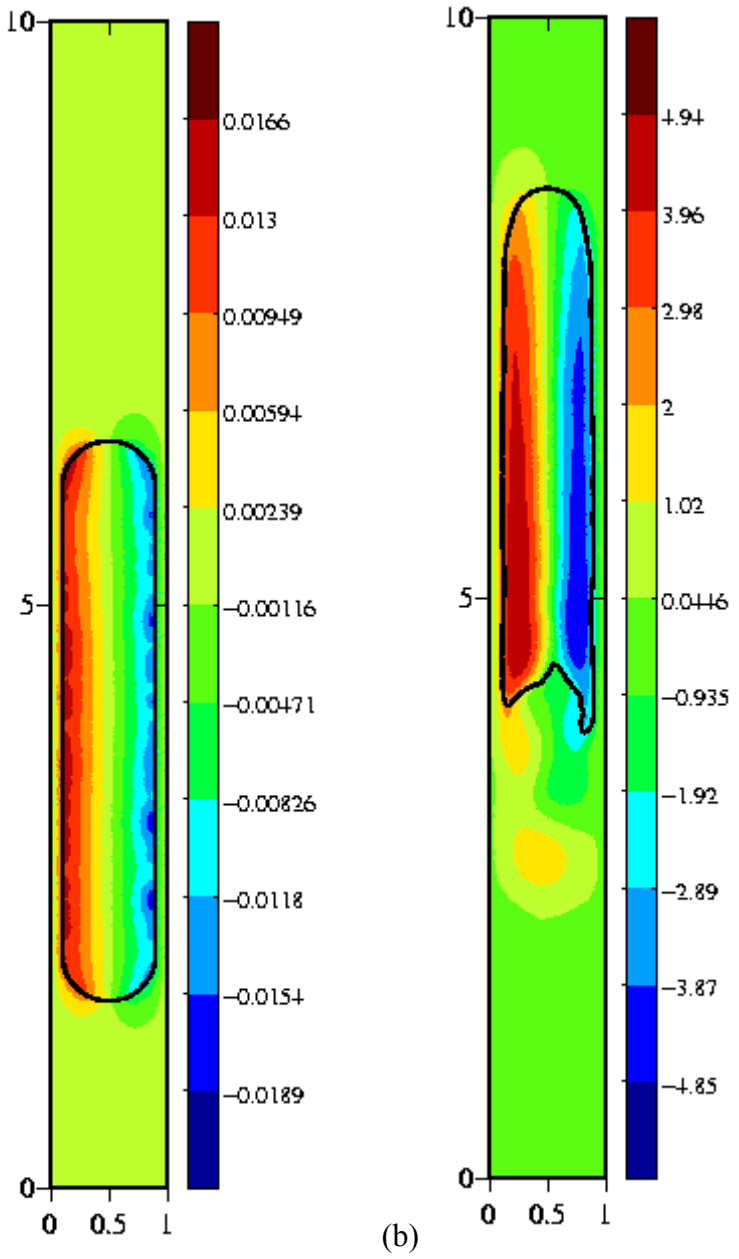

Figure 22. The direct numerical approach is used to simulate the motion of an air bubble rising in a two-dimensional channel filled with a liquid of viscosity 1.0 CGS units. The channel width is 1 cm and the bubble length is approximately 4 cm. The initial bubble width is 0.8 cm. The steady state bubble shape and streamlines are shown. (a) t = 0.001 (b) t = 0.01.

In the level set method, the interface position is not explicitly tracked, but is defined to be the zero level set of a smooth function ϕ, which is assumed to be the signed distance from the interface. Along the interface it is assumed to be zero. In order to track the interface, the level set function is advected according the velocity field. One of the attractive features of this approach is that it is relatively easy to implement in both two and three dimensions. In fact, an algorithm developed for two dimensions can be easily

generalized to three dimensions. Also, the method does not require any special treatment when a front splits into two or when two fronts merge.

Our level set code is fully 3D; unlike previous numerical approaches (Mao et all 1990, Bugg et al 1998) it is not restricted to axisymmetric flow. This code can be used to address all of the questions posed above.

XII Appendix A -Experimental facilities

The Minnesota laboratory has two horizontal 1" diameter × 240" long pipelines; one is equipped for simultaneous injection of water and oil and the other is equipped for studies of pipelining of bitumen froth. The froth line is jacketed in a plastic tube in which cooling water can be circulated. A vertical 0.48D vertical U loop, 180" high is used to study vertical up and down flow. Many measuring devices are available for our use, such as high-speed and high-resolution video cameras, analytical software for image processing and a wide range of rheometers. We plan to use these lines in studies of frictional heating of core-annular flow. We will be comparing data from the Minnesota lab with data from Syncrude's 36" commercial line.

For studies of Taylor bubbles we have constructed a 2" vertical transparent bubble column 10 meters high (figure A.1). The frequency controller can deliver water flow rates from 0.3 m/s to 1.3 m/s.

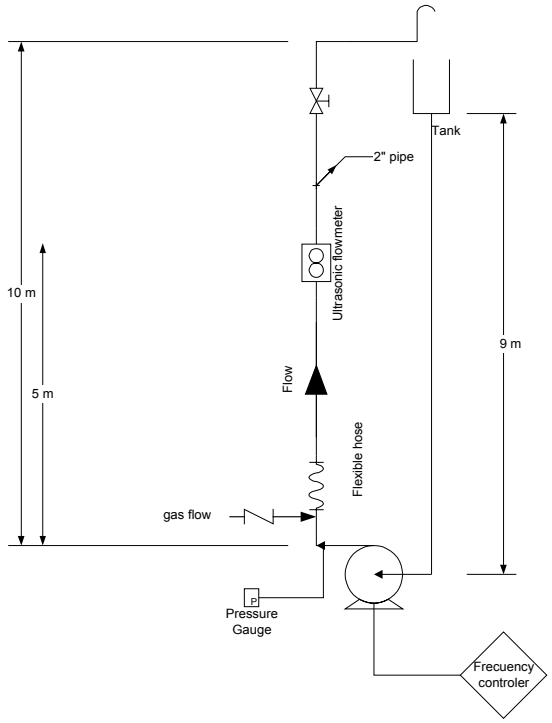

Figure A.1. (right) Bubble column schematic.

The Minnesota lab is not equipped to do experiments on gas-heavy oil flow. The oils are environmentally unfriendly and the pipelines are expensive. We are going to carry out the experiments on heavy oils with viscosities from 130 to 1200 cp at the experimental facility of PDVSA / Intevep in Los Teques, VZ. Their D = 2" horizontal flow loop is 1253D total length, 835D entrance region and 250D test section which is transparent and fully instrumented. The loop is to run with $V_{SL} < 3$ m/s and $V_{SG} < 10$ m/s (see figure A.2).

The experimental apparatus is shown in figure A.3. It consists of a transparent acrylic column with an inside diameter of 3 in. and a total height of approximately 2.5m. At the bottom of the column a transparent acrylic box is connected. The box has a hemispherical cup held above an injection nozzle. This nozzle is connected to a syringe using tubing. In order to obtain the desired bubble volume air is added into the cup, by injecting air repeatedly with the small syringe. The bubble is released by inverting the cup. This mechanism allows the formation of small bubbles (0.8 ml) and Taylor bubbles (300 ml).

To measure the bubble's velocity, the rising bubble is recorded with a high speed video camera NAC HSV 1000, which acquires 500 to 1000 frames per second. This video is digitized and processed by a program developed in PDVSA Intevep using the IMAQ Vision for LabView.

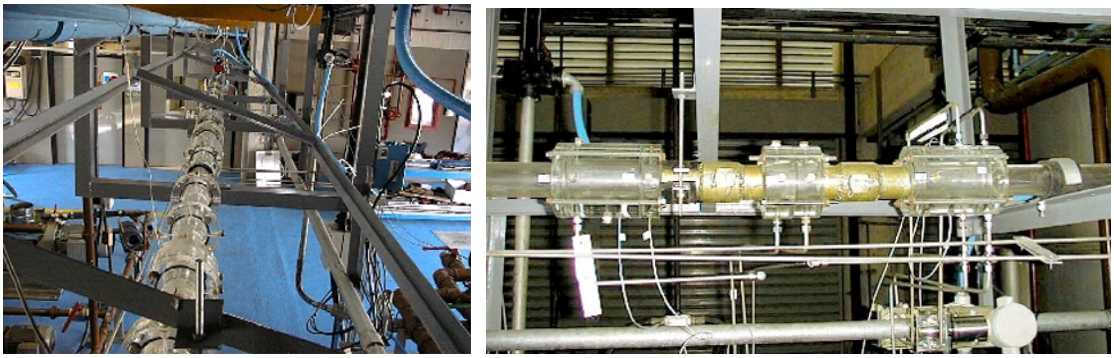

Figure A.2. Horizontal flow loop in Venezuela laboratory.1253D total length, 2 in., 835D entrance region, 250D test section. Fully transparent test section, fully instrumented and advance Scada with slug tracking. V_{SL} *< 3 m/s and* V_{SG} *< 10 m/s,* μ_0 *= 134, 481, 754, 1180 cp.*

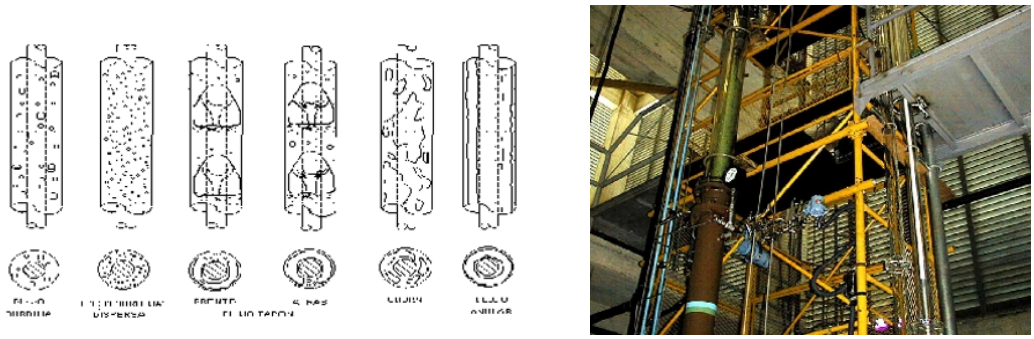

Figure A.3. Vertical flow loop in Venezuela laboratory. 65 ft. long, annulus I.D. 3", internal rod 1". QL = 30-4000 BPD, QG = 1.2-1200 MSCF/D. μ_0 *= 134, 481, 754, 1180 cp. Fully transparent test section, fully instrumented and advance Scada.*

XIII Appendix B – Shear stress transport (SST) turbulence model

Consider two concentric immiscible fluids flowing down an infinite horizontal pipeline. We assume that the core is axisymmetric with interfacial waves that are periodic along the flow direction; the pressure in periodic fully developed flows can be expressed as

$$P(x,r) = -\beta x + p(x,r)\,, \tag{B-1}$$

where β is a mean pressure gradient and $p(x,r)$ represents the periodic part of the whole pressure P and behaves in periodic fashion from module to module. The term βx indicates the general pressure drop along the flow direction.

The continuity equation and Navier-Stoke equation for the unsteady incompressible flow in cylindrical coordinate can be written as follows:

continuity

$$\frac{\partial}{\partial x}(\rho u)+\frac{1}{r}\frac{\partial}{\partial r}(r\rho v)=0\,, \tag{B-2}$$

x-momentum

$$\rho\left[\frac{\partial u}{\partial t}+u\frac{\partial u}{\partial x}+v\frac{\partial u}{\partial r}\right]=\beta-\frac{\partial p}{\partial x}+\frac{\partial}{\partial x}\left(\mu_{eff}\left(2\frac{\partial u}{\partial x}\right)\right)+\frac{1}{r}\frac{\partial}{\partial r}\left(r\mu_{eff}\left(\frac{\partial v}{\partial x}+\frac{\partial u}{\partial r}\right)\right)-\rho\frac{2}{3}\frac{\partial k}{\partial x}, \tag{B-3}$$

r-momentum

$$\rho\left[\frac{\partial v}{\partial t}+u\frac{\partial v}{\partial x}+v\frac{\partial v}{\partial r}\right]=-\frac{\partial p}{\partial r}+\frac{\partial}{\partial x}\left(\mu_{eff}\left(\frac{\partial v}{\partial x}+\frac{\partial u}{\partial r}\right)\right)+\frac{1}{r}\frac{\partial}{\partial r}\left(r\mu_{eff}\left(2\frac{\partial v}{\partial r}\right)\right)-2\mu_{eff}\frac{v}{r^2}-\rho\frac{2}{3}\frac{\partial k}{\partial x}, \tag{B-4}$$

where

$$\mu_{eff}=\mu+\mu_T\,,\qquad \mu_T=\rho\frac{0.31k}{\max(0.31\omega;\Omega F_2)}\,,$$

and Ω is the absolute value of the vorticity.

The turbulent kinetic energy equation and the dissipation rate equation are obtained from Menter's shear stress transport model (F. R. Menter 1994). The SST model utilizes the original k-ω model of Wilcox in the inner region of the boundary layer and switches to the standard k-ε model in the outer region of the boundary layer and in free shear flows. In the dissipation rate equation, the function F_1 is designed to be one in the near wall region (activating the original model) and zero away from the surface (activating the transformed model). Then the turbulent kinetic energy and the dissipation rate equation modified by SST model are written as

turbulent kinetic energy

$$\rho\left[\frac{\partial k}{\partial t}+u\frac{\partial k}{\partial x}+v\frac{\partial k}{\partial r}\right]=P_k+\frac{\partial}{\partial x}\left((\mu+\sigma_k\mu_T)\frac{\partial k}{\partial x}\right)+\frac{1}{r}\frac{\partial}{\partial r}\left(r(\mu+\sigma_k\mu_T)\frac{\partial k}{\partial r}\right)-\beta^*\rho k\omega\,, \tag{B-5}$$

dissipation rate

$$\rho\left[\frac{\partial \omega}{\partial t}+u\frac{\partial \omega}{\partial x}+v\frac{\partial \omega}{\partial r}\right]=\frac{\partial}{\partial x}\left((\mu+\sigma_\omega\mu_T)\frac{\partial \omega}{\partial x}\right)+\rho\frac{\gamma}{\mu_T}P_k-\beta\rho\omega^2$$

$$+\frac{1}{r}\frac{\partial}{\partial r}\left(r(\mu+\sigma_\omega\mu_T)\frac{\partial \omega}{\partial r}\right)+2(1-F_1)\rho\sigma_{\omega 2}\frac{1}{\omega}\frac{\partial k}{\partial x}\frac{\partial \omega}{\partial x}+2(1-F_1)\rho\sigma_{\omega 2}\frac{1}{\omega}\frac{\partial k}{\partial r}\frac{\partial \omega}{\partial r}\,, \tag{B-6}$$

where

$$P_k = \mu_T \left(2 \left(\left(\frac{\partial u}{\partial x} \right)^2 + \left(\frac{\partial v}{\partial r} \right)^2 + \left(\frac{v}{r} \right)^2 \right) + \left(\frac{\partial v}{\partial x} + \frac{\partial u}{\partial r} \right)^2 \right).$$

Let ϕ_1 represent a constant in the original k-ω model ($\sigma_{k1},\ldots$), ϕ_2 a constant in the transformed k-ε model ($\sigma_{k2},\ldots$). The corresponding constant ϕ of the new model ($\sigma_{k},\ldots$) is given as follows:

$$\Phi = F_1 \Phi_1 + (1 - F_1) \Phi_2 . \tag{B-7}$$

The constants of set 1 (ϕ_1) and set 2 (ϕ_2) are

$$\sigma_{k1} = 0.85,\ \sigma_{w1} = 0.5,\ \beta_1 = 0.075,\ \kappa = 0.41,\quad \gamma_1 = \beta_1 / \beta^* - \sigma_{\omega 1} \kappa^2 / \sqrt{\beta^*},$$

$$\sigma_{k2} = 1.0,\ \sigma_{w2} = 1.856,\ \beta_2 = 0.0828,\ \beta^* = 0.09,\quad \gamma_1 = \beta_2 / \beta^* - \sigma_{\omega 2} \kappa^2 / \sqrt{\beta^*},$$

and F_1 and F_2 are given by

$$F_1 = \tanh(\arg_1^4),\ \arg_1 = \min\left[\max\left(\frac{\sqrt{k}}{0.09\omega y}; \frac{500\mu}{y^2 \rho \omega} \right); \frac{4\rho\sigma_{\omega 2} k}{CD_{k\omega} y^2} \right],$$

$$CD_{k\omega} = \max\left(2\rho\sigma_{\omega 2} \frac{1}{\omega} \frac{\partial k}{\partial x_j} \frac{\partial \omega}{\partial x_j}; 10^{-20} \right),\ F_2 = \tanh(\arg_2^2),\ \arg_2 = \max\left(\frac{\sqrt{k}}{0.09\omega y}; \frac{500\mu}{y^2 \rho \omega} \right),$$

where y is the distance to the next surface.

XIV References

The first ten references are listed in section II on page 4 of the text.

---

[11] D.D. Joseph & Y. Renardy, 1992. *Fundamentals of Two-Fluid Dynamics. Part II*, IAM4

[12] D.D. Joseph, R. Bai, K.P. Chen & Y. Renardy, 1997. Core-annular flows, *Annular Rev. Fluid Mech*. 21, 65-90. This paper gives an overview of the issues posed by the science and technology of transporting heavy oil in a sheath of lubricating water. It touches on measures of energy efficiency, industrial experiences, fouling, stability, models of levitation and future direction.

[13] V. Kruka, 1977. Method for establishing Core-Flow in Water-in-Oil Emulsions or dispersions Canadian patent granted to Shell Canada, No. 1008108.

[14] O. Neiman, K. Sury, D.D. Joseph, R. Bai and C. Grant, 1999. Process for pumping bitumen froth through a pipeline, US Patent 5,988,198.

[15] O Neiman . 1986. Froth pipelining tests. *Syncrude Canada Research and Development Progress Report.* **15**(1):373-407.

[16] DD Joseph, R Bai, C Mata, K Sury & C Grant, 1999. Self-lubricated transport of bitumen froth, *J. Fluid Mech*. **386**, 127-148.

[17] R Bai, K Kelkar, DD Joseph, 1996. Direct simulation of interfacial waves in a high-viscosity-ratio and axisymmetric core-annular flow. *J. Fluid Mech.* **327**, 1-34.

[18] R Bai, K Chen and DD Joseph, 1992. Lubricated pipelining: stability of core-annular flow. Part 5, experiments and comparison with theory. *J. Fluid Mech.* **240**, 97-142.

[19] J Li, Y Renardy, 1999. Direct simulation of unsteady axisymmetric core-annular flow with high viscosity ratio. *J. Fluid Mech.* **391**, 123-149.

[20] R Bai & DD Joseph, 2000. Steady flow and interfacial shapes of a highly viscous dispersed phase, *Int. J. Multiphase Flow,* **26**, 1469-1491.

[21] T Ko, HG Choi, R Bai and DD Joseph, 2000. Turbulent wavy core-annular flow simulation using a k-ω turbulence model and finite element method, in progress.

[22] FR Menter, 1994. Two-equation eddy-viscosity turbulence models for engineering applications. *AIAA Journal*, **32**(8), 1598-1605.

[23] R Chokshi, Z Schmidt, D Doty. May 1996. *Experimental Study and the Development of a Mechanistic Model for Two-Phase flow Through Vertical Tubing*. SPE 35676. Western Regional Meeting, Alaska, pp 255-267.

[24] L Gómez, O Shoham, Z Schmidt, R Chokshi, A. Brown, T. Northug October 1999. *A Unified Model for Steady Two-Phase Flow in Wellbores and Pipelines*. SPE 56520, SPE Annual Technical Conference and Exhibition, Houston, Texas, pp 307-320.

[25] J.M. Mandhane, G.A. Gregory and K. Aziz, 1974, A flow pattern map for gas-liquid flow in horizontal pipes. *Int. J. Multiphase Flow* **1**, 537-551.

[26] PY Lin & TJ Hanratty, 1987. Effect of pipe diameter on flow patterns for air-water flow in horizontal pipes, *Int. J. Multiphase Flow,* **13**(4), 549-563.

[27] G.B. Wallis and J.E. Dobson, 1973. The onset of slugging in horizontal stratified air-water flow. *Int. J. Multiphase Flow,* **1**, 173-193.

[28] C.J. Crowley, G.H. Wallis and J.J. Barry, 1992. Validation of a one-dimensional wave model for the stratified-to-slug flow regime transition, with consequences for wave growth and slug frequency. *Int. J. Multiphase Flow*. **18**(2), 249-271.

[29] DD Joseph and TY Liao, 1994. Potential flows of viscous and viscoelastic fluids, *J. Fluid Mech*. **265**, 1-23.

[30] D.D. Joseph, J. Belanger and G.S. Beavers, 1999. Breakup of a liquid drop suddenly exposed to a high-speed airstream, *Int. J. Multiphase Flow* **25**, 1263-1303.

[31] DD Joseph, TS Lundgren, T Funada, 2000. Viscous Potential Flow Analysis of Kelvin-Helmholtz Instability, *http://www.aem.umn.edu/people/faculty/joseph/.*

[32] T Funada and DD Joseph, 2000. Viscous potential flow analysis of Kelvin-Helmholz instability in a channel, Submitted to *Int. J. Multiphase Flow;* also *http://www.aem.umn.edu/people/faculty/joseph/.*

[33] D. Barnea, and Y. Taitel, 1993. Kelvin-Helmholtz stability criteria for stratified flow: viscous versus non-viscous (inviscid) approaches, *Int. J. Multiphase Flow* **19**, 639-649.

[34] N. Andritsos, L. Williams and T.J. Hanratty, 1989. Effect of liquid viscosity on the stratified-slug transition in horizontal pipe flow. *Int. J. Multiphase Flow,* **15**, 877-892.

[35] N. Andritsos and T.J. Hanratty, 1987. Interfacial instabilities for horizontal gas-liquid flows in pipelines, *Int. J. Multiphase Flow,* **13**, 583-603.

[36] Al Sharki and TJ Hanratty, 2000. Effect of drag reducing polymers on annular gas-liquid flow in a horizontal pipe, *Int. J. Multiphase Flow*, to appear.

[37] CJ Manfield, C Lawrence and G Hewitt, 1999. Drag reduction with additives in multiphase flow: a literature survey. *Multiphase Science and Technology*, **11**, 197-221.

[38] T Min, JY Yoo, H Choi and DD Joseph, 2000. Direct numerical simulation of turbulent drag reduction by polymer additive. *DFD00 meeting of the American Physical Society*. To be published.

[39] Y. Taitel and A.E. Dukler, 1976. A model for predicting flow regime transitions in horizontal and near horizontal gas-liquid flow. *AIChE J.,* **22**, 47-55.

[40] E.S. Kordyban and T. Ranov, 1970. Mechanism of slug formation in horizontal two-phase flow. *Trans. ASME J. Basic Engng.,* **92**, 857-864.

[41] G Iooss and DD Joseph, 1990. *Elementary Stability and Bifurcation Theory*. Springer, 2nd edition.

[42] RM Davies and GI Taylor 1950. The mechanism of large bubbles rising through liquids in tubes, *Proceedings of the Royal Society*, **200**(A), 375-390.

[43] G.K. Batchelor 1967, *An Introduction to Fluid Dynamics*, Cambridge University Press, page 477.

[44] ET White and RH Beardmore 1962. The velocity of rise of single cylindrical air bubbles through liquids contained in vertical tubes. *Chem. Eng. Sci.* **17**, 351-361.

[45] RAS Brown 1965. The mechanics of large gas bubbles in tubes, I. Bubble velocities in stagnant liquids. The Canadian Journal of Chemical Engineering, October, pp 217.

[46] EF Caetano, O. Shoham and JP Brill, 1992. Upward vertical two-phase flow through an annulus--Part I: Single-phase friction factor, Taylor bubble rise velocity, and flow pattern prediction. *J. Energy Resources Tech*., **114**, 1.

[47] EW Radar, AT Bourgoyne and RH Ward, 1975. Factors affecting bubble rise velocity gas kicks. *J. Pet. Tech.* **27**, 571-584.

[48] JR Grace and D Harrison, 1967. The influence of bubble shape on the rising velocities of large buble, *Chemical Engineering Science.* **22**, 1337-1347.

[49] ET White and RH Beardmore, 1962. The velocity of rise of single cylindrical air bubbles through liquids contained in vertical tubes. *Chem. Eng. Sci.* **17**, 351-361.

[50] Z-S Mao and AE Dukler, 1990. The motion of Taylor bubbles in vertical tubes. I. A numerical simulation for the shape and rise velocity of Taylor bubbles in stagnant and flowing liquids. *J. Comp. Phys.* **91**, 132-160.

[51] JD Bugg, K Mack and KS Rezkallah, 1998. a numerical model of Taylor bubbles rising through stagnant liquids in vertical tubes, *Int. J. Multiphase Flow,* **24**(2), 271-281.